analysis of risk factors for intrahepatic recurrence. Ann Surg 2003;237:536–543.
11. Portolani N, Coniglio A, Ghidoni S, et al. Early and late recurrence after liver resection for hepatocellular carcinoma: prognostic and therapeutic implications. Ann Surg 2006;243:229–235.
12. Capussotti L, Ferrero A, Viganò L, et al. Portal hypertension: contraindication to liver surgery? World J Surg 2006;30:992–999.
13. Yamamoto J, Kosuge T, Takayama T, et al. Recurrence of hepatocellular carcinoma after surgery. Br J Surg 1996;83:1219–1222.
14. Llovet JM, Fuster J, Bruix J. Intention-to-treat analysis of surgical treatment for early hepatocellular carcinoma: resection versus transplantation. Hepatology 1999;30:1434–1440.
15. Arii S, Yamaoka Y, Futagawa S, et al. Results of surgical and nonsurgical treatment for small-sized hepatocellular carcinomas: a retrospective and nationwide survey in Japan. Hepatology 2000;32:1224–1229.
16. Bruix J, Castells A, Bosch J, et al. Surgical resection of hepatocellular carcinoma in cirrhotic patients: prognostic value of preoperative portal pressure. Gastroenterology 1996;111:1018–1022.
17. Llovet JM, Brú C, Bruix J. Prognosis of hepatocellular carcinoma: the BCLC staging classification. Semin Liver Dis 1999;19:329–338.
18. Makuuchi M, Kosuge T, Takayama T, et al. Surgery for small liver cancers. Semin Surg Oncol 1993;9:298–304.
19. Imamura H, Sano K, Sugawara Y, et al. Assessment of hepatic reserve for indication of hepatic resection: decision tree incorporating indocyanine green test. J Hepatobiliary Pancreat Surg 2005;12:16–22.
20. Lee SG, Hwang S. How I do it: assessment of hepatic functional reserve for indication of hepatic resection. J Hepatobiliary Pancreat Surg 2005;12:38–43.
21. Bruix J, Sherman M, Llovet JM, et al. Clinical management of hepatocellular carcinoma. Conclusions of the Barcelona-2000 EASL conference. J Hepatol 2001;35:421–430.
22. Bruix J, Sherman M. Management of hepatocellular carcinoma. Hepatology 2005;42:1208–1236.
23. Bezerra AS, D'Ippolito G, Faintuch S, et al. Determination of splenomegaly by CT: is there a place for a single measurement? AJR Am J Roentgenol 2005;184:1510–1513.
24. Pugh RN, Murray-Lyon IM, Dawson JL, et al. Transection of the oesophagus for bleeding oesophageal varices. Br J Surg 1973;60:646–649.
25. Torzilli G, Makuuchi M, Inoue K, et al. No-mortality liver resection for hepatocellular carcinoma in cirrhotic and noncirrhotic patients: is there a way? A prospective analysis of our approach. Arch Surg 1999;134:984–992.
26. Japanese Research Society for Portal Hypertension. The general rules for recording endoscopic findings on esophageal varices. Jpn J Surg 1980;10:84–87.
27. Sugawara Y, Yamamoto J, Shimada K, et al. Splenectomy in patients with hepatocellular carcinoma and hypersplenism. J Am Coll Surg 2000;190:446–450.
28. Hassab MA. Gastroesophageal decongestion and splenectomy in the treatment of esophageal varices in bilharzial cirrhosis: further studies with a report on 355 operations. Surgery 1967;61:169–176.
29. Takayama T, Makuuchi M, Hirohashi S, et al. Early hepatocellular carcinoma as an entity with a high rate of surgical cure. Hepatology 1998;28:1241–1246.
30. Torzilli G, Minagawa M, Takayama T, et al. Accurate preoperative evaluation of liver mass lesions without fine-needle biopsy. Hepatology 1999;30:889–893.
31. Nakayama A, Imamura H, Matsuyama Y, et al. Value of lipiodol computed tomography and digital subtraction angiography in the era of helical biphasic computed tomography as preoperative assessment of hepatocellular carcinoma. Ann Surg 2001;234:56–62.
32. Makuuchi M, Hasegawa H, Yamazaki S. Ultrasonically guided subsegmentectomy. Surg Gynecol Obstet 1985;161:346–350.
33. Kokudo N, Bandai Y, Imanishi H, et al. Management of new hepatic nodules detected by intraoperative ultrasonography during hepatic resection for hepatocellular carcinoma. Surgery 1996;119:634–640.
34. Minagawa M, Makuuchi M, Takayama T, et al. Selection criteria for repeat hepatectomy in patients with recurrent hepatocellular carcinoma. Ann Surg 2003;238:703–710.
35. Bruix J, Hessheimer AJ, Forner A, et al. New aspects of diagnosis and therapy of hepatocellular carcinoma. Oncogene 2006;25:3848–3856.
36. Cillo U, Bassanello M, Vitale A, et al. The critical issue of hepatocellular carcinoma prognostic classification: which is the best tool available? J Hepatol 2004;40:124–131.
37. Bismuth H, Chiche L, Adam R, et al. Liver resection versus transplantation for hepatocellular carcinoma in cirrhotic patients. Ann Surg 1993;218:145–151.
38. Mazzaferro V, Regalia E, Doci R, et al. Liver transplantation for the treatment of small hepatocellular carcinoma in patients with cirrhosis. N Engl J Med 1996;334:693–699.
39. Adam R, McMaster P, O'Grady JG, et al. Evolution of liver transplantation in Europe: report of the European Liver Transplant Registry. Liver Transpl 2003;9:1231–1243.
40. The 2006 OPTN/SRTR annual report: transplantation data 1996–2005. Available at http://www.optnorg/AR2006. Accessed July 5, 2007.
41. Torzilli G, Donadon N, Marconi M, et al. Hepatectomy for hepatocellular carcinoma in stage B and C of Barcelona-Clinic-Liver-Cancer Classification: results of a prospective analysis. Arch Surg (in press).

Received September 7, 2007. Accepted February 28, 2008.

Address requests for reprints to: Norihiro Kokudo, MD, PhD, Hepato-Biliary-Pancreatic Surgery Division, Department of Surgery, Graduate School of Medicine, University of Tokyo, 7-3-1 Hongo, Bunkyo-ku, Tokyo 113-8655, Japan. e-mail: kokudo-2su@h.u-tokyo.ac.jp; fax: (81) 3-5800-8844.

Supported by a grant from the Kanae Foundation for Life & Socio-medical Science, a grant from the Public Trust Surgery Research Fund, a grant from the Japanese Clinical Oncology Fund, and a grant from the Public Trust Haraguchi Memorial Cancer Research Fund in Japan, and a Grant-in-aid for Scientific Research from the Ministry of Education, Culture, Sports, Science and Technology of Japan (grant 18790955).

frontiers in MICROBIOLOGY

REVIEW ARTICLE
published: 07 February 2012
doi: 10.3389/fmicb.2012.00038

Morphogenesis of infectious hepatitis C virus particles

Tetsuro Suzuki*

Department of Infectious Diseases, Hamamatsu University School of Medicine, Hamamatsu, Japan

Edited by:
Akio Adachi, The University of Tokushima Graduate School, Japan

Reviewed by:
MinKyung Yi, University of Texas Medical Branch at Galveston, USA
Michael Schindler, Helmholtz Zentrum München – German Research Center for Environmental Health, Germany
Hideki Tani, National Institute of Infectious Diseases, Japan

***Correspondence:**
Tetsuro Suzuki, Department of Infectious Diseases, Hamamatsu University School of Medicine, 1-20-1 Handayama, Higashi-ku, Hamamatsu 431-3192, Japan.
e-mail: tesuzuki@hama-med.ac.jp

More than 170 million individuals are currently infected with hepatitis C virus (HCV) worldwide and are at continuous risk of developing chronic liver disease. Since a cell culture system enabling relatively efficient propagation of HCV has become available, an increasing number of viral and host factors involved in HCV particle formation have been identified. Association of the viral Core, which forms the capsid with lipid droplets appears to be prerequisite for early HCV morphogenesis. Maturation and release of HCV particles is tightly linked to very-low-density lipoprotein biogenesis. Although expression of Core as well as E1 and E2 envelope proteins produces virus-like particles in heterologous expression systems, there is increasing evidence that non-structural viral proteins and p7 are also required for the production of infectious particles, suggesting that HCV genome replication and virion assembly are closely linked. Advances in our understanding of the various molecular mechanisms by which infectious HCV particles are formed are summarized.

Keywords: hepatitis C virus, assembly, lipid droplet, VLDL

INTRODUCTION

Hepatitis C virus (HCV) infection is a major cause of chronic hepatitis, liver cirrhosis, and hepatocellular carcinoma. HCV is primarily transmitted by blood-borne routes, including shared needles and transfused blood products. The WHO estimates that a minimum of 2–3% of the world's population is chronically infected with HCV (Wasley and Alter, 2000). Despite the fact that HCV is targeted by innate, cellular, and humoral immune mechanisms, it establishes long-standing persistent infection in a majority of the people that it infects (Pawlotsky, 2006). HCV belongs to the genus *Hepacivirus* within the Flaviviridae family. The virus forms small round-shaped particles ranging from 50 to 80 nm in diameter. The mature HCV virion is thought to consist of a nucleocapsid, an outer envelope composed of E1 and E2 viral proteins, and a lipid membrane. HCV particles isolated from the sera of infected patients demonstrate heterogeneity in their density. Density gradient analyses have shown that viral RNA exists within both low- and high-density fractions (Andre et al., 2005), and that the low-density fractions contain lipoproteins that associate with apolipoprotein B (ApoB), apolipoprotein E (ApoE), triglycerides, and cholesterol, as well as viral structural proteins (Thomssen et al., 1992; Andre et al., 2002; Maillard et al., 2006; Nielsen et al., 2006). Only the low-density fraction derived from HCV-positive human serum exhibits high infectivity in chimpanzees (Bradley et al., 1991; Beach et al., 1992). Since the establishment of a robust tissue culture infection system using strain HCV JFH-1 (Lindenbach et al., 2005; Wakita et al., 2005; Zhong et al., 2005), the entire HCV lifecycle has been studied and the biophysical properties of the viral particles produced using the HCVcc cell culture system have been characterized. Most viral RNA-containing particles secreted from HCV-infected cells are poorly infectious and fractionate at high densities such as ~1.14 g/mL, while highly infectious HCVcc are found within low-density fractions of ~1.10 g/mL (Lindenbach et al., 2005).

Here, we provide a general account of our current understanding of the HCV lifecycle and a review of recent studies focusing on the morphogenesis of HCV particles within cell culture systems.

HCV GENOME ORGANIZATION AND PROTEIN SYNTHESIS

Hepatitis C virus is a positive-stranded RNA virus, and its ~9.6-kb genome contains an open reading frame encoding a polyprotein of ~3000 amino acids (aa) flanked by untranslated regions (UTRs) at both ends. Six genotypes have been reported based on HCV genome sequence variations (Simmonds, 1996). The UTRs are highly structured sequences encompassing critical cis-active RNA elements essential for genome replication and translation. The 5′ UTR, which is ~341 nucleotides (nt) in length, contains an internal ribosomal entry site, which is a prerequisite for cap-independent translation of viral RNA, from which four highly structured domains (I–IV) are produced (Bukh et al., 1992; Tsukiyama-Kohara et al., 1992; Wang et al., 1993; Honda et al., 1996; Friebe et al., 2001). The 3′ UTR varies between 200 and 235 nt in length, including a short variable region, as well as a poly(U/UC) tract with an average length of 80 nt which is considered crucial for RNA replication, and a virtually invariant 98-nt X-tail region (Tanaka et al., 1995; Ito and Lai, 1999; Friebe and Bartenschlager, 2002; Yi and Lemon, 2003).

The genome is translated into a single precursor polyprotein, which is processed by cellular and viral proteases into 10 structural and non-structural proteins (Core, E1, E2, p7, NS2, NS3, NS4A, NS4B, NS5A, and NS5B; **Figure 1**). HCV proteins derived from the amino-terminal third of the precursor include Core, E1 and E2 structural proteins. A crucial function of Core protein is assembly of the viral nucleocapsid. The aa sequence of this protein is well conserved among different HCV strains compared to other HCV proteins. The non-structural (NS) proteins NS3-NS5B are thought to assemble into a membrane-associated HCV RNA replicase complex. NS3 functions as serine protease, RNA helicase, and NTPase.

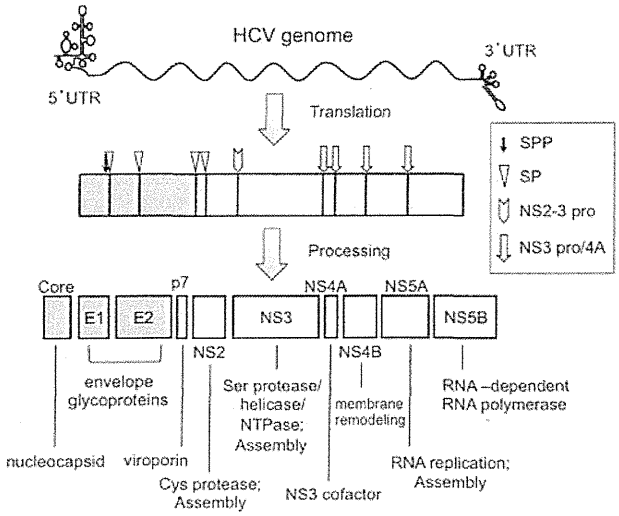

FIGURE 1 | The HCV genome and polyprotein. The RNA genome comprises a 9.6-kb RNA of plus strand polarity. Post-translational cleavages by SPP (signal peptide peptidase), SP (signal peptidase), NS2-3 pro (NS2–NS3 cysteine protease), and NS3 pro/4A (NS3 serine protease and NS4A complex) lead to the production of functional HCV proteins. Functions of each protein in the viral lifecycle are indicated below the open reading frame.

NS4A serves as a cofactor for NS3 and is involved in targeting NS3 to the ER membrane (Wolk et al., 2000). NS4B plays a role in the remodeling of host-cell membranes, probably to generate a site for replicase assembly. NS5A is also thought to play an important but undefined role in viral RNA replication. NS5B functions as an RNA-dependent RNA polymerase. The role of HCV NS proteins in assembly of the infectious virion is described below.

CORE PROTEIN AND NUCLEOCAPSID FORMATION

The Core is 191 aa in length and consists of three distinct predicted domains: an N-terminal domain that is two-thirds hydrophilic, a C-terminal domain that is one-third hydrophobic, and a short signal peptide sequence of the downstream protein E1. The precursor Core is cleaved between Core and E1 by a host signal peptidase. A C-terminal membrane-anchor of the Core is further cleaved by a signal peptide peptidase. The mature Core is estimated to be 177–179 aa (Ogino et al., 2004; Okamoto et al., 2004). Maturation of the Core by a signal peptide peptidase is required for virion production (Okamoto et al., 2008; Targett-Adams et al., 2008). Biophysical techniques have been used to demonstrate that the mature Core is a dimeric alpha-helical protein (Boulant et al., 2005). Its aa sequence is highly conserved among different HCV strains, compared with other HCV proteins. Thus, Core is used in most serologic assays since anti-core antibodies are highly prevalent among HCV-infected individuals.

Core has been detected in a number of subcellular compartments. Core protein is found on ER membranes, on the surface of lipid droplets (LDs), on the mitochondrial outer membrane, and to some extent, in the nucleus (Moradpour et al., 1996; Barba et al., 1997; Moriya et al., 1998; Yasui et al., 1998; Hope et al., 2002; Suzuki et al., 2005). Following is a proposed mechanism of translocation of Core to membranes within the ER network such as LDs (McLauchlan et al., 2002; Schwer et al., 2004). After being processed by a signal peptide peptidase, a large part of the Core remains within cytoplasmic leaflets of the ER membrane due to preservation of the original transmembrane domain. The cytoplasmic leaflets then swell as lipid accumulates between the two membrane leaflets. As a result, the Core is translocated along with part of the ER membrane to the surface of a nascent LD before the droplet buds off the ER. The proteasome-dependent degradation pathway then participates in post-translational modification of the Core (Suzuki et al., 2001, 2009; Moriishi et al., 2003, 2007, 2010; Shirakura et al., 2007). Ubiquitin ligase E6AP and proteasome activator PA28gamma are key regulators in determining the fate of the Core, and thereby play a role in virus production (Shirakura et al., 2007; Moriishi et al., 2010).

The ~120 N-terminal residues of the Core protein (domain I) contain multiple positively charged residues that are implicated in RNA binding and homo-oligomerization. It is therefore likely that this domain is a prerequisite for assembly of the HCV nucleocapsid (Kunkel et al., 2001; Klein et al., 2004, 2005; Majeau et al., 2004). It has been shown that a region extending from aa 72 to 91 is responsible for auto-oligomerization of Core (Nakai et al., 2006). Although conclusive data for direct packaging of the HCV genome into the viral capsid is lacking, the viral RNA sequence of the Core protein through to the NS2 region appears not to contain a cis-acting packaging signal. A subgenomic replicon RNA carrying the NS3–NS5B region can be encapsidated in the viral trans-packaging system (Ishii et al., 2008; Steinmann et al., 2008; Adair et al., 2009; Masaki et al., 2010). In addition, the RNA sequence encoding the first 62 aa of Core contains highly conserved structures including two stem-loops that are important for RNA translation/replication (McMullan et al., 2007). Domain II (aa ~120–170) is predicted to form two alpha-helices that enable Core to associate with membrane proteins and lipids. Domain II is involved in targeting of Core to LDs. It has been proposed that domain II folding occurs in a membrane environment and is critical for the folding of domain I (Boulant et al., 2005). In addition, a cysteine residue at aa 128 of domain II creates a disulfide bond to produce a Core protein dimer that is required for particle formation (Kushima et al., 2010). Domain III, pertaining to ~20 residues at the C-terminal, is highly hydrophobic and serves as a signal sequence for E1. Although little is known about the molecular mechanisms governing assembly of Core into nucleocapsids, comprehensive mutagenesis studies have enabled identification of various aa residues which are essential for HCV morphogenesis (Murray et al., 2007; Alsaleh et al., 2010; Kopp et al., 2010).

INVOLVEMENT OF OTHER HCV PROTEINS IN ASSEMBLY

Two N-glycosylated envelope proteins E1 and E2 are exposed on the surface of the virus as a heterodimer that mediates viral attachment to host-cell receptors and facilitates virus entry (Op De Beeck et al., 2004; Vieyres et al., 2010). During their synthesis, E1 and E2 assemble as non-covalent heterodimers. Ectodomains of E1 and E2 are translocated inside the ER lumen and their transmembrane domains are inserted in the membrane of this compartment. E1 contains four to five N-linked glycans and E2

has 11 N-glycosylation sites. HCV glycans, which are thought to contain a mixture of complex and high mannose side-chain, play a role in envelope protein folding and formation of the E1/E2 complexes. The importance of incorporating N-linked glycans of the envelope proteins into infectious virions has been demonstrated (Helle et al., 2010). A recent study has shown that HCV infection activates the ER-associated degradation pathway, which in turn controls the fate of E1 and E2 and modulates virus production (Saeed et al., 2011).

A role of viral NS proteins in HCV production was first suggested following the observation that JFH-1-derived NS proteins are required to generate infectious virus from intra- and inter-genotype chimeric constructs (Lindenbach et al., 2005; Pietschmann et al., 2006). Evidence supporting a role of NS2, NS3, and NS5A in the assembly or release of infectious HCV has come from mutational analyses (Jones et al., 2007; Miyanari et al., 2007; Appel et al., 2008; Jirasko et al., 2008; Ma et al., 2008; Masaki et al., 2008; Tellinghuisen et al., 2008).

NS5A is a hydrophilic phosphoprotein which plays a key role in viral RNA replication and is involved in modulation of cell signaling pathways and the interferon response (Huang et al., 2007). NS5A is associated with membrane mediated by a unique amphipathic alpha helix which is located at its N-terminus (Moradpour et al., 2005), and part of NS5A localizes to LDs when expressed alone or as the viral polyprotein (Shi et al., 2002). Experiments based on HCV genomes containing mutated NS5A have shown that some mutants result in failure of association of NS5A with LDs and failure of production of infectious particles (Miyanari et al., 2007). Further studies have revealed that the C-terminal region of NS5A plays a key role in HCV production (Appel et al., 2008; Masaki et al., 2008; Tellinghuisen et al., 2008). Substitutions at a serine cluster of the NS5A C-terminus (aa 2428, 2430, and 2433) which have no impact on viral RNA replication, have been observed to inhibit the interaction between NS5A and Core, thereby suggesting that an association between NS5A and Core might be involved in virus production (Masaki et al., 2008). Structural analyses have shown that the N-terminal region of NS5A forms a "claw-like" dimer, which might accommodate RNA and interact with viral and cellular proteins and membranes (Huang et al., 2005; Tellinghuisen et al., 2005). It appears that recruitment of NS5A to LDs, thereby enabling interaction with the Core, is crucial for virion assembly. One can imagine that newly synthesized HCV RNA bound to NS5A is released from the replication complex-containing membrane compartment and can then be captured by Core through interaction with the C-terminal region of NS5A at the surface of LDs or LD-associated membranes. Consequently, viral RNA becomes encapsidated and virion assembly proceeds (**Figure 2**). In this regard, a study has revealed an interaction between NS5A and ApoE, suggesting that recruitment of ApoE by NS5A is important for the assembly and release of HCV particles (Benga et al., 2010).

NS3–NS4A is another component of the viral replication complex that exhibits serine protease, as well as RNA helicase and RNA-stimulated NTPase activity, necessary for viral RNA replication. It is now apparent that NS3–NS4A also contributes to viral assembly (Yi et al., 2007; Ma et al., 2008; Han et al., 2009; Phan et al., 2011). A previous study has provided genetic evidence that

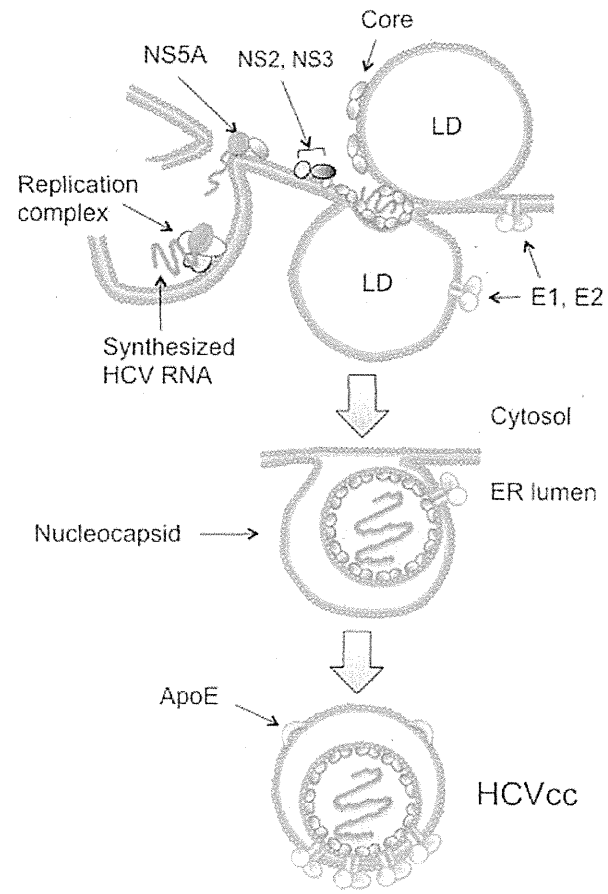

FIGURE 2 | Proposed model for assembly of HCV particles. After accumulation of synthesized genome RNA and the viral proteins, the HCV particles are assembled in an ER-related compartment in close connection with the VLDL pathway. The viral replication complex, which is composed of NS3–NS5B and host factors, is a specialized structure protected by cellular membrane. Newly synthesized viral RNAs are recruited to surfaces of lipid droplet (LD), where ER membrane is associated, possibly via interaction between NS5A and Core. Thus, the RNAs enable to associate with Core, thereby proceeding encapsidation and nucleocapsid formation. The nucleocapsid is presumably inserted into the lipid core of the luminal LD and buds into the ER lumen with incorporation of E1 and E2. HCV–lipoprotein particle formed is then released from the cells.

two major subdomains of the NS3 helicase, one demonstrating NTPase activity and the other associated with RNA binding, are involved in the early stages of virion assembly, independent of their roles as enzymes (Ma et al., 2008). A separate investigation has revealed a contribution of the acidic domain of NS4A to both RNA replication and virus assembly (Phan et al., 2011).

NS2 is a cysteine protease composed of a highly hydrophobic N-terminal membrane binding domain which forms either three or four transmembrane helices that insert into the ER membrane. NS2 also contains a C-terminal globular and cytosolic protease subdomain, that produce zinc-stimulated NS2/3 autoprotease activity together with the N-terminal one-third of NS3.

Mutagenesis of NS2 has identified regions or residues that are important for infectious virus production (Jones et al., 2007; Yi et al., 2007, 2009; Jirasko et al., 2008, 2010; Dentzer et al., 2009; Phan et al., 2009; Ma et al., 2011; Popescu et al., 2011). For example, mutations involving the dimer interface of the protease region or the C-terminus of NS2 impair the production of infectious HCV, while the catalytic activity of NS2 is not required for viral assembly. Genetic and biochemical data demonstrate that NS2 is possibly involved in multiple interactions with both HCV structural and NS proteins including E1–E2, p7, NS3, and NS5A, suggesting that NS2 has a role in recruiting these viral proteins to sites in close proximity with LDs. Alternatively, it may act as a scaffold promoting virus assembly (Jirasko et al., 2010; Ma et al., 2011; Stapleford and Lindenbach, 2011).

p7 is a 63-aa polypeptide located between E2 and NS2, and is a membrane-spanning protein localized within the ER. p7 belongs to a class of viral permeability-altering proteins termed "viroporins." It behaves as an ion channel when reconstituted into artificial lipid membranes. Although p7 is not required for viral RNA replication in cell culture, the protein is essential for HCV infectivity in chimpanzees (Sakai et al., 2003). Subsequent analyses in HCVcc systems have demonstrated that p7 is important for virion production since the introduction of p7 mutations, such as mutations in the basic residues required for its ion channel activity, impair virus production (Jones et al., 2007; Steinmann et al., 2007; Brohm et al., 2009). Although it is not yet clear whether the ion channel function of the protein is needed for virus assembly, a recent study has demonstrated that p7 functions as an H^+ channel in native intracellular membranes and links p7-induced pH changes to the production of infectious intracellular virions (Wozniak et al., 2010).

ROLE OF LIPID METABOLISM IN HCV ASSEMBLY

HCVcc contained within low-density fractions from the culture supernatant of virus-producing cells displays greater specific infectivity than virus in high-density fractions (Lindenbach et al., 2005; Ogawa et al., 2009). Looking also at the behavior of HCV circulating within the sera of infected hosts, it may be that low-density virus associates with lipid and very-low-density lipoprotein (VLDL) and/or low-density lipoprotein (LDL). Furthermore, HCV particles obtained from virus-infected animals, such as chimpanzees and chimeric mice transplanted with human hepatocytes, demonstrate greater infectivity than virus produced in cell cultures. The virus populations derived from these infected animals have been observed to fractionate into lower density fractions than a major population of HCVcc (Lindenbach et al., 2006). Interestingly, the association of cholesterol and sphingolipid with HCV virions has been shown to play a critical role in viral infectivity (Kapadia et al., 2007; Aizaki et al., 2008; Voisset et al., 2008). Depletion of cholesterol and sphingomyelin from HCV virions inhibits the infectivity of HCVcc (Aizaki et al., 2008). The structural requirement of virion-associated cholesterol for infectivity, as well as its influence on buoyant density, and the association of apolipoprotein with HCV, has been further demonstrated by Yamamoto et al. (2011).

There is accumulating evidence that assembly and secretion of HCV particles are associated with the VLDL assembly pathway. Lipoproteins can be differentiated on the basis of their density, which is affected by lipid content and the types of apolipoprotein they contain. VLDLs are large triglyceride-rich lipoproteins (30–80 nm in diameter) containing cholesterol, cholesteryl esters, ApoB, and other minor apolipoprotein(s). VLDLs carry triglyceride from the liver to peripheral tissue for storage and to provide a source of energy. Triglyceride availability and the size of intracellular triglyceride pools are important regulatory factors in the regulation of VLDL production. In addition, the microsomal triglyceride transfer protein (MTP), which is responsible for the transport of triglyceride and cholesteryl esters across ER membranes, is required for VLDL assembly. Purified membrane vesicles containing the HCV replication complex are enriched with ApoB, MTP, and ApoE (Huang et al., 2007). Moreover, agents that inhibit VLDL assembly also inhibit HCV secretion from cells producing infectious virus (Chang et al., 2007; Huang et al., 2007; Gastaminza et al., 2008). ApoB, ApoC1, and ApoE have been observed to associate with HCV particles during viral morphogenesis in the HCVcc system (Chang et al., 2007; Meunier et al., 2008; Jiang and Luo, 2009; Owen et al., 2009; Benga et al., 2010). Furthermore, ApoE depletion suppresses the production of infectious HCV (Chang et al., 2007; Jiang and Luo, 2009; Owen et al., 2009; Benga et al., 2010; Hishiki et al., 2010). These findings demonstrate that ApoE is important for HCV infectivity, suggesting that HCV virions are assembled as ApoE-enriched lipoprotein particles. A study in which virion-associated cholesterol was depleted and replenished with exogenous sterol analogs has provided evidence that virion-associated cholesterol contributes to the interaction between HCV and ApoE (Yamamoto et al., 2011). ApoE is a polymorphic protein with three major isoforms: ApoE2, ApoE3, and ApoE4. Differential roles of ApoE isoforms on infectious HCV production have been revealed: ectopic expression of ApoE3 or ApoE4 enables recovery of infectious HCV, while ApoE2 has little influence on virus production (Hishiki et al., 2010). Not surprisingly, ApoE2 demonstrates significantly less LDL receptor binding activity than ApoE3 and ApoE4 (Davignon et al., 1988).

Hepatitis C virus may utilize the assembly and secretion of VLDL to exit cells. In fact, secretion of E1 and E2 within the culture supernatant is reduced by treatment with MTP inhibitors (Icard et al., 2009). VLDL maturation occurs by acquisition of lipids from LDs either in the ER lumen or in the Golgi apparatus. It is likely that HCV envelopment takes place in a lipid-enriched microdomain at the ER membrane where luminal LDs or VLDL precursors are generated (**Figure 2**), in keeping with evidence of increased cholesterol content among HCV particles compared to host-cell membranes (Aizaki et al., 2008).

Neutral lipids such as triglycerides and cholesterol esters are stored within cytosolic LD in cells. LD is thought to be a source of neutral lipid for metabolism and membrane synthesis. Neutral lipids form the LD core and are surrounded by an outer layer of amphipathic lipids such as phospholipids and cholesterol. LD is thought to be surrounded by a lipid monolayer. Prior to the availability of a tissue culture system for virion production, HCV Core was shown to associate with ER membranes and on the surface of LDs in heterologous expression systems in mammalian cells (Moradpour et al., 1996; Barba et al., 1997). Early studies of cells infected with HCV JFH-1 indicate that Core is detectable at the ER

and on the surface of LDs in association with the ER (Rouille et al., 2006). Core associates with LDs in a time-dependent manner and disruption of this process coincides with a loss of virion production (Boulant et al., 2007). It has subsequently been demonstrated that LDs are directly involved in the production of infectious HCV and that Core recruits viral non-structural proteins as well as the replication complex to the LD-associated membranes, suggesting that the association between Core and LDs is required at a certain stage of HCV morphogenesis (Miyanari et al., 2007). Fluorescent labeling and functional imaging of Core in living cells has recently been used to visualize Core during HCV assembly (Counihan et al., 2011). Core has been observed to move to the surface of large, immobile LDs soon after protein translation. Core has also been observed in motile puncta that travel along microtubules. Diacylglycerol acyltransferases (DGATs) catalyze the final step of triglyceride synthesis and are crucial for LD biogenesis. A study has revealed that DGAT1 interacts with Core and is required for trafficking of the Core to LD. Disrupting translocation of the Core to LD by inhibiting DGAT1 activity or through knockdown of the DGAT1 gene impairs virus production (Herker et al., 2010). Thus, there is now increasing evidence that LDs play a central role in the production of infectious HCV and participate in virus assembly. However, one study has demonstrated that, while Core derived from HCV JFH-1 is strongly associated with cytoplasmic LDs, minimal Core from a HCV clone with higher assembly efficiency is detectable on LDs (Shavinskaya et al., 2007). Thus, it remains debatable whether HCV assembly is initiated on the surface of LDs or at sites where ER cisternae are in contact with LDs. Based on the current evidence, a model for nucleocapsid formation following the initial phase of assembly is demonstrated in **Figure 2**. Two potential models to explain HCV nucleocapsid formation, including the model shown in **Figure 2**, have been proposed by Bartenschlager et al. (2011).

FUTURE PERSPECTIVES

Evidence regarding the assembly of infectious HCV particles has accumulated over the past several years since the availability of HCVcc systems. A variety of key factors in HCV morphogenesis have been identified, including the requirement for components of the VLDL biosynthetic machinery and viral NS proteins. However, there are still essential questions to be answered. Detailed mechanisms pertaining to nucleotide formation, genome packaging, and the way in which HCV interacts with the lipoprotein/VLDL pathway, as well as the precise role of various NS proteins and p7 in HCV assembly, remain unclear. Structural studies will be important to clarify the exact composition of the HCV virion, as well as similarities and differences between HCVcc generated in Huh-7-derived cells and the "lipoviroparticles" produced by circulating virus within infected individuals.

ACKNOWLEDGMENTS

The author is grateful to Masayoshi Fukasawa (National Institute of Infectious Diseases, Department of Biochemistry and Cell Biology) for his helpful discussion. The author would also like to thank all members of the National Institute of Infectious Diseases, Department of Virology II, as well as the Hamamatsu University School of Medicine, Department of Infectious Diseases, for their technical support and valuable discussion and advice. This work was supported in part by a Grant-in-Aid from the Ministry of Health, Labor, and Welfare of Japan, and by a Grant-in-Aid from the Ministry of Education, Culture, Sports, Science, and Technology of Japan.

REFERENCES

Adair, R., Patel, A. H., Corless, L., Griffin, S., Rowlands, D. J., and Mccormick, C. J. (2009). Expression of hepatitis C virus (HCV) structural proteins in trans facilitates encapsidation and transmission of HCV subgenomic RNA. *J. Gen. Virol.* 90, 833–842.

Aizaki, H., Morikawa, K., Fukasawa, M., Hara, H., Inoue, Y., Tani, H., Saito, K., Nishijima, M., Hanada, K., Matsuura, Y., Lai, M. M. C., Miyamura, T., Wakita, T., and Suzuki, T. (2008). Critical role of virion-associated cholesterol and sphingolipid in hepatitis C virus infection. *J. Virol.* 82, 5715–5724.

Alsaleh, K., Delavalle, P.-Y., Pillez, A., Duverlie, G., Descamps, V., Rouille, Y., Dubuisson, J., and Wychowski, C. (2010). Identification of basic amino acids at the N-terminal end of the core protein that are crucial for hepatitis C virus infectivity. *J. Virol.* 84, 12515–12528.

Andre, P., Komurian-Pradel, F., Deforges, S., Perret, M., Berland, J. L., Sodoyer, M., Pol, S., Brechot, C., Paranhos-Baccala, G., and Lotteau, V. (2002). Characterization of low- and very-low-density hepatitis C virus RNA-containing particles. *J. Virol.* 76, 6919–6928.

Andre, P., Perlemuter, G., Budkowska, A., Brechot, C., and Lotteau, V. (2005). Hepatitis C virus particles and lipoprotein metabolism. *Semin. Liver Dis.* 25, 93–104.

Appel, N., Zayas, M., Miller, S., Krijnse-Locker, J., Schaller, T., Friebe, P., Kallis, S., Engel, U., and Bartenschlager, R. (2008). Essential role of domain III of nonstructural protein 5A for hepatitis C virus infectious particle assembly. *PLoS Pathog.* 4, e1000035. doi:10.1371/journal.ppat.1000035

Barba, G., Harper, F., Harada, T., Kohara, M., Goulinet, S., Matsuura, Y., Eder, G., Schaff, Z., Chapman, M. J., Miyamura, T., and Brechot, C. (1997). Hepatitis C virus core protein shows a cytoplasmic localization and associates to cellular lipid storage droplets. *Proc. Natl. Acad. Sci. U.S.A.* 94, 1200–1205.

Bartenschlager, R., Penin, F., Lohmann, V., and Andre, P. (2011). Assembly of infectious hepatitis C virus particles. *Trends Microbiol.* 19, 95–103.

Beach, M. J., Meeks, E. L., Mimms, L. T., Vallari, D., Ducharme, L., Spelbring, J., Taskar, S., Schleicher, J. B., Krawczynski, K., and Bradley, D. W. (1992). Temporal relationships of hepatitis C virus RNA and antibody responses following experimental infection of chimpanzees. *J. Med. Virol.* 36, 226–237.

Benga, W. J. A., Krieger, S. E., Dimitrova, M., Zeisel, M. B., Parnot, M., Lupberger, J., Hildt, E., Luo, G., Mclauchlan, J., Baumert, T. F., and Schuster, C. (2010). Apolipoprotein E interacts with hepatitis C virus nonstructural protein 5A and determines assembly of infectious particles. *Hepatology* 51, 43–53.

Boulant, S., Targett-Adams, P., and Mclauchlan, J. (2007). Disrupting the association of hepatitis C virus core protein with lipid droplets correlates with a loss in production of infectious virus. *J. Gen. Virol.* 88, 2204–2213.

Boulant, S., Vanbelle, C., Ebel, C., Penin, F., and Lavergne, J.-P. (2005). Hepatitis C virus core protein is a dimeric alpha-helical protein exhibiting membrane protein features. *J. Virol.* 79, 11353–11365.

Bradley, D., Mccaustland, K., Krawczynski, K., Spelbring, J., Humphrey, C., and Cook, E. H. (1991). Hepatitis C virus: buoyant density of the factor VIII-derived isolate in sucrose. *J. Med. Virol.* 34, 206–208.

Brohm, C., Steinmann, E., Friesland, M., Lorenz, I. C., Patel, A., Penin, F., Bartenschlager, R., and Pietschmann, T. (2009). Characterization of determinants important for hepatitis C virus p7 function in morphogenesis by using trans-complementation. *J. Virol.* 83, 11682–11693.

Bukh, J., Purcell, R. H., and Miller, R. H. (1992). Sequence analysis of the 5' noncoding region of hepatitis C virus. *Proc. Natl. Acad. Sci. U.S.A.* 89, 4942–4946.

Chang, K.-S., Jiang, J., Cai, Z., and Luo, G. (2007). Human apolipoprotein e is required for infectivity and production of hepatitis C virus in cell culture. *J. Virol.* 81, 13783–13793.

Counihan, N. A., Rawlinson, S. M., and Lindenbach, B. D. (2011). Trafficking of hepatitis C virus core protein during virus particle assembly. *PLoS Pathog.* 7, e1002302. doi:10.1371/journal.ppat.1002302

Davignon, J., Gregg, R. E., and Sing, C. F. (1988). Apolipoprotein E polymorphism and atherosclerosis. *Arteriosclerosis* 8, 1–21.

Dentzer, T. G., Lorenz, I. C., Evans, M. J., and Rice, C. M. (2009). Determinants of the hepatitis C virus nonstructural protein 2 protease domain required for production of infectious virus. *J. Virol.* 83, 12702–12713.

Friebe, P., and Bartenschlager, R. (2002). Genetic analysis of sequences in the 3' nontranslated region of hepatitis C virus that are important for RNA replication. *J. Virol.* 76, 5326–5338.

Friebe, P., Lohmann, V., Krieger, N., and Bartenschlager, R. (2001). Sequences in the 5' nontranslated region of hepatitis C virus required for RNA replication. *J. Virol.* 75, 12047–12057.

Gastaminza, P., Cheng, G., Wieland, S., Zhong, J., Liao, W., and Chisari, F. V. (2008). Cellular determinants of hepatitis C virus assembly, maturation, degradation, and secretion. *J. Virol.* 82, 2120–2129.

Han, Q., Xu, C., Wu, C., Zhu, W., Yang, R., and Chen, X. (2009). Compensatory mutations in NS3 and NS5A proteins enhance the virus production capability of hepatitis C reporter virus. *Virus Res.* 145, 63–73.

Helle, F., Vieyres, G., Elkrief, L., Popescu, C.-I., Wychowski, C., Descamps, V., Castelain, S., Roingeard, P., Duverlie, G., and Dubuisson, J. (2010). Role of N-linked glycans in the functions of hepatitis C virus envelope proteins incorporated into infectious virions. *J. Virol.* 84, 11905–11915.

Herker, E., Harris, C., Hernandez, C., Carpentier, A., Kaehlcke, K., Rosenberg, A. R., Farese, R. V. Jr., and Ott, M. (2010). Efficient hepatitis C virus particle formation requires diacylglycerol acyltransferase-1. *Nat. Med.* 16, 1295–1298.

Hishiki, T., Shimizu, Y., Tobita, R., Sugiyama, K., Ogawa, K., Funami, K., Ohsaki, Y., Fujimoto, T., Takaku, H., Wakita, T., Baumert, T. F., Miyanari, Y., and Shimotohno, K. (2010). Infectivity of hepatitis C virus is influenced by association with apolipoprotein E isoforms. *J. Virol.* 84, 12048–12057.

Honda, M., Brown, E. A., and Lemon, S. M. (1996). Stability of a stem-loop involving the initiator AUG controls the efficiency of internal initiation of translation on hepatitis C virus RNA. *RNA* 2, 955–968.

Hope, R. G., Murphy, D. J., and Mclauchlan, J. (2002). The domains required to direct core proteins of hepatitis C virus and GB virus-B to lipid droplets share common features with plant oleosin proteins. *J. Biol. Chem.* 277, 4261–4270.

Huang, H., Sun, F., Owen, D. M., Li, W., Chen, Y., Gale, M. Jr., and Ye, J. (2007). Hepatitis C virus production by human hepatocytes dependent on assembly and secretion of very low-density lipoproteins. *Proc. Natl. Acad. Sci. U.S.A.* 104, 5848–5853.

Huang, L., Hwang, J., Sharma, S. D., Hargittai, M. R. S., Chen, Y., Arnold, J. J., Raney, K. D., and Cameron, C. E. (2005). Hepatitis C virus nonstructural protein 5A (NS5A) is an RNA-binding protein. *J. Biol. Chem.* 280, 36417–36428.

Icard, V., Diaz, O., Scholtes, C., Perrin-Cocon, L., Ramiere, C., Bartenschlager, R., Penin, F., Lotteau, V., and Andre, P. (2009). Secretion of hepatitis C virus envelope glycoproteins depends on assembly of apolipoprotein B positive lipoproteins. *PLoS ONE* 4, e4233. doi:10.1371/journal.pone.0004233

Ishii, K., Murakami, K., Hmwe, S. S., Zhang, B., Li, J., Shirakura, M., Morikawa, K., Suzuki, R., Miyamura, T., Wakita, T., and Suzuki, T. (2008). Trans-encapsidation of hepatitis C virus subgenomic replicon RNA with viral structure proteins. *Biochem. Biophys. Res. Commun.* 371, 446–450.

Ito, T., and Lai, M. M. (1999). An internal polypyrimidine-tract-binding protein-binding site in the hepatitis C virus RNA attenuates translation, which is relieved by the 3'-untranslated sequence. *Virology* 254, 288–296.

Jiang, J., and Luo, G. (2009). Apolipoprotein E but not B is required for the formation of infectious hepatitis C virus particles. *J. Virol.* 83, 12680–12691.

Jirasko, V., Montserret, R., Appel, N., Janvier, A., Eustachi, L., Brohm, C., Steinmann, E., Pietschmann, T., Penin, F., and Bartenschlager, R. (2008). Structural and functional characterization of nonstructural protein 2 for its role in hepatitis C virus assembly. *J. Biol. Chem.* 283, 28546–28562.

Jirasko, V., Montserret, R., Lee, J. Y., Gouttenoire, J., Moradpour, D., Penin, F., and Bartenschlager, R. (2010). Structural and functional studies of nonstructural protein 2 of the hepatitis C virus reveal its key role as organizer of virion assembly. *PLoS Pathog.* 6, e1001233. doi:10.1371/journal.ppat.1001233

Jones, C. T., Murray, C. L., Eastman, D. K., Tassello, J., and Rice, C. M. (2007). Hepatitis C virus p7 and NS2 proteins are essential for production of infectious virus. *J. Virol.* 81, 8374–8383.

Kapadia, S. B., Barth, H., Baumert, T., Mckeating, J. A., and Chisari, F. V. (2007). Initiation of hepatitis C virus infection is dependent on cholesterol and cooperativity between CD81 and scavenger receptor B type I. *J. Virol.* 81, 374–383.

Klein, K. C., Dellos, S. R., and Lingappa, J. R. (2005). Identification of residues in the hepatitis C virus core protein that are critical for capsid assembly in a cell-free system. *J. Virol.* 79, 6814–6826.

Klein, K. C., Polyak, S. J., and Lingappa, J. R. (2004). Unique features of hepatitis C virus capsid formation revealed by de novo cell-free assembly. *J. Virol.* 78, 9257–9269.

Kopp, M., Murray, C. L., Jones, C. T., and Rice, C. M. (2010). Genetic analysis of the carboxy-terminal region of the hepatitis C virus core protein. *J. Virol.* 84, 1666–1673.

Kunkel, M., Lorinczi, M., Rijnbrand, R., Lemon, S. M., and Watowich, S. J. (2001). Self-assembly of nucleocapsid-like particles from recombinant hepatitis C virus core protein. *J. Virol.* 75, 2119–2129.

Kushima, Y., Wakita, T., and Hijikata, M. (2010). A disulfide-bonded dimer of the core protein of hepatitis C virus is important for virus-like particle production. *J. Virol.* 84, 9118–9127.

Lindenbach, B. D., Evans, M. J., Syder, A. J., Wolk, B., Tellinghuisen, T. L., Liu, C. C., Maruyama, T., Hynes, R. O., Burton, D. R., Mckeating, J. A., and Rice, C. M. (2005). Complete replication of hepatitis C virus in cell culture. *Science* 309, 623–626.

Lindenbach, B. D., Meuleman, P., Ploss, A., Vanwolleghem, T., Syder, A. J., Mckeating, J. A., Lanford, R. E., Feinstone, S. M., Major, M. E., Leroux-Roels, G., and Rice, C. M. (2006). Cell culture-grown hepatitis C virus is infectious in vivo and can be recultured in vitro. *Proc. Natl. Acad. Sci. U.S.A.* 103, 3805–3809.

Ma, Y., Anantpadma, M., Timpe, J. M., Shanmugam, S., Singh, S. M., Lemon, S. M., and Yi, M. (2011). Hepatitis C virus NS2 protein serves as a scaffold for virus assembly by interacting with both structural and nonstructural proteins. *J. Virol.* 85, 86–97.

Ma, Y., Yates, J., Liang, Y., Lemon, S. M., and Yi, M. (2008). NS3 helicase domains involved in infectious intracellular hepatitis C virus particle assembly. *J. Virol.* 82, 7624–7639.

Maillard, P., Huby, T., Andreo, U., Moreau, M., Chapman, J., and Budkowska, A. (2006). The interaction of natural hepatitis C virus with human scavenger receptor SR-BI/Cla1 is mediated by ApoB-containing lipoproteins. *FASEB J.* 20, 735–737.

Majeau, N., Gagne, V., Boivin, A., Bolduc, M., Majeau, J.-A., Ouellet, D., and Leclerc, D. (2004). The N-terminal half of the core protein of hepatitis C virus is sufficient for nucleocapsid formation. *J. Gen. Virol.* 85, 971–981.

Masaki, T., Suzuki, R., Murakami, K., Aizaki, H., Ishii, K., Murayama, A., Date, T., Matsuura, Y., Miyamura, T., Wakita, T., and Suzuki, T. (2008). Interaction of hepatitis C virus nonstructural protein 5A with core protein is critical for the production of infectious virus particles. *J. Virol.* 82, 7964–7976.

Masaki, T., Suzuki, R., Saeed, M., Mori, K.-I., Matsuda, M., Aizaki, H., Ishii, K., Maki, N., Miyamura, T., Matsuura, Y., Wakita, T., and Suzuki, T. (2010). Production of infectious hepatitis C virus by using RNA polymerase I-mediated transcription. *J. Virol.* 84, 5824–5835.

McLauchlan, J., Lemberg, M. K., Hope, G., and Martoglio, B. (2002). Intramembrane proteolysis promotes trafficking of hepatitis C virus core protein to lipid droplets. *EMBO J.* 21, 3980–3988.

McMullan, L. K., Grakoui, A., Evans, M. J., Mihalik, K., Puig, M., Branch, A. D., Feinstone, S. M., and Rice, C. M. (2007). Evidence for a functional RNA element in the hepatitis C virus core gene. *Proc. Natl. Acad. Sci. U.S.A.* 104, 2879–2884.

Meunier, J.-C., Russell, R. S., Engle, R. E., Faulk, K. N., Purcell, R. H., and Emerson, S. U. (2008). Apolipoprotein c1 association with hepatitis C virus. *J. Virol.* 82, 9647–9656.

Miyanari, Y., Atsuzawa, K., Usuda, N., Watashi, K., Hishiki, T., Zayas, M., Bartenschlager, R., Wakita, T., Hijikata, M., and Shimotohno, K. (2007). The lipid droplet is an important organelle for hepatitis C virus production. *Nat. Cell Biol.* 9, 1089–1097.

Moradpour, D., Brass, V., and Penin, F. (2005). Function follows form: the structure of the N-terminal domain of HCV NS5A. *Hepatology* 42, 732–735.

Moradpour, D., Wakita, T., Tokushige, K., Carlson, R. I., Krawczynski, K., and Wands, J. R. (1996). Characterization of three novel monoclonal antibodies against hepatitis C virus core protein. *J. Med. Virol.* 48, 234–241.

Moriishi, K., Mochizuki, R., Moriya, K., Miyamoto, H., Mori, Y., Abe, T., Murata, S., Tanaka, K., Miyamura, T., Suzuki, T., Koike, K., and Matsuura, Y. (2007). Critical role of PA28gamma in hepatitis C virus-associated steatogenesis and hepatocarcinogenesis. *Proc. Natl. Acad. Sci. U.S.A.* 104, 1661–1666.

Moriishi, K., Okabayashi, T., Nakai, K., Moriya, K., Koike, K., Murata, S., Chiba, T., Tanaka, K., Suzuki, R., Suzuki, T., Miyamura, T., and Matsuura, Y. (2003). Proteasome activator PA28gamma-dependent nuclear retention and degradation of hepatitis C virus core protein. *J. Virol.* 77, 10237–10249.

Moriishi, K., Shoji, I., Mori, Y., Suzuki, R., Suzuki, T., Kataoka, C., and Matsuura, Y. (2010). Involvement of PA28gamma in the propagation of hepatitis C virus. *Hepatology* 52, 411–420.

Moriya, K., Fujie, H., Shintani, Y., Yotsuyanagi, H., Tsutsumi, T., Ishibashi, K., Matsuura, Y., Kimura, S., Miyamura, T., and Koike, K. (1998). The core protein of hepatitis C virus induces hepatocellular carcinoma in transgenic mice. *Nat. Med.* 4, 1065–1067.

Murray, C. L., Jones, C. T., Tassello, J., and Rice, C. M. (2007). Alanine scanning of the hepatitis C virus core protein reveals numerous residues essential for production of infectious virus. *J. Virol.* 81, 10220–10231.

Nakai, K., Okamoto, T., Kimura-Someya, T., Ishii, K., Lim, C. K., Tani, H., Matsuo, E., Abe, T., Mori, Y., Suzuki, T., Miyamura, T., Nunberg, J. H., Moriishi, K., and Matsuura, Y. (2006). Oligomerization of hepatitis C virus core protein is crucial for interaction with the cytoplasmic domain of E1 envelope protein. *J. Virol.* 80, 11265–11273.

Nielsen, S. U., Bassendine, M. F., Burt, A. D., Martin, C., Pumeechockchai, W., and Toms, G. L. (2006). Association between hepatitis C virus and very-low-density lipoprotein (VLDL)/LDL analyzed in iodixanol density gradients. *J. Virol.* 80, 2418–2428.

Ogawa, K., Hishiki, T., Shimizu, Y., Funami, K., Sugiyama, K., Miyanari, Y., and Shimotohno, K. (2009). Hepatitis C virus utilizes lipid droplet for production of infectious virus. *Proc. Jpn. Acad. Ser. B Phys. Biol. Sci.* 85, 217–228.

Ogino, T., Fukuda, H., Imajoh-Ohmi, S., Kohara, M., and Nomoto, A. (2004). Membrane binding properties and terminal residues of the mature hepatitis C virus capsid protein in insect cells. *J. Virol.* 78, 11766–11777.

Okamoto, K., Mori, Y., Komoda, Y., Okamoto, T., Okochi, M., Takeda, M., Suzuki, T., Moriishi, K., and Matsuura, Y. (2008). Intramembrane processing by signal peptide peptidase regulates the membrane localization of hepatitis C virus core protein and viral propagation. *J. Virol.* 82, 8349–8361.

Okamoto, K., Moriishi, K., Miyamura, T., and Matsuura, Y. (2004). Intramembrane proteolysis and endoplasmic reticulum retention of hepatitis C virus core protein. *J. Virol.* 78, 6370–6380.

Op De Beeck, A., Voisset, C., Bartosch, B., Ciczora, Y., Cocquerel, L., Keck, Z., Foung, S., Cosset, F.-L., and Dubuisson, J. (2004). Characterization of functional hepatitis C virus envelope glycoproteins. *J. Virol.* 78, 2994–3002.

Owen, D. M., Huang, H., Ye, J., and Gale, M. Jr. (2009). Apolipoprotein E on hepatitis C virion facilitates infection through interaction with low-density lipoprotein receptor. *Virology* 394, 99–108.

Pawlotsky, J. M. (2006). Hepatitis C virus population dynamics during infection. *Curr. Top. Microbiol. Immunol.* 299, 261–284.

Phan, T., Beran, R. K. F., Peters, C., Lorenz, I. C., and Lindenbach, B. D. (2009). Hepatitis C virus NS2 protein contributes to virus particle assembly via opposing epistatic interactions with the E1-E2 glycoprotein and NS3-NS4A enzyme complexes. *J. Virol.* 83, 8379–8395.

Phan, T., Kohlway, A., Dimberu, P., Pyle, A. M., and Lindenbach, B. D. (2011). The acidic domain of hepatitis C virus NS4A contributes to RNA replication and virus particle assembly. *J. Virol.* 85, 1193–1204.

Pietschmann, T., Kaul, A., Koutsoudakis, G., Shavinskaya, A., Kallis, S., Steinmann, E., Abid, K., Negro, F., Dreux, M., Cosset, F.-L., and Bartenschlager, R. (2006). Construction and characterization of infectious intragenotypic and intergenotypic hepatitis C virus chimeras. *Proc. Natl. Acad. Sci. U.S.A.* 103, 7408–7413.

Popescu, C.-I., Callens, N., Trinel, D., Roingeard, P., Moradpour, D., Descamps, V., Duverlie, G., Penin, F., Heliot, L., Rouille, Y., and Dubuisson, J. (2011). NS2 protein of hepatitis C virus interacts with structural and non-structural proteins towards virus assembly. *PLoS Pathog.* 7, e1001278. doi:10.1371/journal.ppat.1001278

Rouille, Y., Helle, F., Delgrange, D., Roingeard, P., Voisset, C., Blanchard, E., Belouzard, S., Mckeating, J., Patel, A. H., Maertens, G., Wakita, T., Wychowski, C., and Dubuisson, J. (2006). Subcellular localization of hepatitis C virus structural proteins in a cell culture system that efficiently replicates the virus. *J. Virol.* 80, 2832–2841.

Saeed, M., Suzuki, R., Watanabe, N., Masaki, T., Tomonaga, M., Muhammad, A., Kato, T., Matsuura, Y., Watanabe, H., Wakita, T., and Suzuki, T. (2011). Role of the endoplasmic reticulum-associated degradation (ERAD) pathway in degradation of hepatitis C virus envelope proteins and production of virus particles. *J. Biol. Chem.* 286, 37264–37273.

Sakai, A., Claire, M. S., Faulk, K., Govindarajan, S., Emerson, S. U., Purcell, R. H., and Bukh, J. (2003). The p7 polypeptide of hepatitis C virus is critical for infectivity and contains functionally important genotype-specific sequences. *Proc. Natl. Acad. Sci. U.S.A.* 100, 11646–11651.

Schwer, B., Ren, S., Pietschmann, T., Kartenbeck, J., Kaehlcke, K., Bartenschlager, R., Yen, T. S. B., and Ott, M. (2004). Targeting of hepatitis C virus core protein to mitochondria through a novel C-terminal localization motif. *J. Virol.* 78, 7958–7968.

Shavinskaya, A., Boulant, S., Penin, F., Mclauchlan, J., and Bartenschlager, R. (2007). The lipid droplet binding domain of hepatitis C virus core protein is a major determinant for efficient virus assembly. *J. Biol. Chem.* 282, 37158–37169.

Shi, S. T., Polyak, S. J., Tu, H., Taylor, D. R., Gretch, D. R., and Lai, M. M. C. (2002). Hepatitis C virus NS5A colocalizes with the core protein on lipid droplets and interacts with apolipoproteins. *Virology* 292, 198–210.

Shirakura, M., Murakami, K., Ichimura, T., Suzuki, R., Shimoji, T., Fukuda, K., Abe, K., Sato, S., Fukasawa, M., Yamakawa, Y., Nishijima, M., Moriishi, K., Matsuura, Y., Wakita, T., Suzuki, T., Howley, P. M., Miyamura, T., and Shoji, I. (2007). E6AP ubiquitin ligase mediates ubiquitylation and degradation of hepatitis C virus core protein. *J. Virol.* 81, 1174–1185.

Simmonds, P. (1996). Virology of hepatitis C virus. *Clin. Ther.* 18 Suppl B, 9–36.

Stapleford, K. A., and Lindenbach, B. D. (2011). Hepatitis C virus NS2 coordinates virus particle assembly through physical interactions with the E1-E2 glycoprotein and NS3-NS4A enzyme complexes. *J. Virol.* 85, 1706–1717.

Steinmann, E., Brohm, C., Kallis, S., Bartenschlager, R., and Pietschmann, T. (2008). Efficient trans-encapsidation of hepatitis C virus RNAs into infectious virus-like particles. *J. Virol.* 82, 7034–7046.

Steinmann, E., Penin, F., Kallis, S., Patel, A. H., Bartenschlager, R., and Pietschmann, T. (2007). Hepatitis C virus p7 protein is crucial for assembly and release of infectious virions. *PLoS Pathog.* 3, e103. doi:10.1371/journal.ppat.0030103

Suzuki, R., Moriishi, K., Fukuda, K., Shirakura, M., Ishii, K., Shoji, I., Wakita, T., Miyamura, T., Matsuura, Y., and Suzuki, T. (2009). Proteasomal turnover of hepatitis C virus core protein is regulated by two distinct mechanisms: a ubiquitin-dependent mechanism and a ubiquitin-independent but PA28gamma-dependent mechanism. *J. Virol.* 83, 2389–2392.

Suzuki, R., Sakamoto, S., Tsutsumi, T., Rikimaru, A., Tanaka, K., Shimoike, T., Moriishi, K., Iwasaki, T., Mizumoto, K., Matsuura, Y., Miyamura, T., and Suzuki, T. (2005). Molecular determinants for subcellular localization of hepatitis C virus core protein. *J. Virol.* 79, 1271–1281.

Suzuki, R., Tamura, K., Li, J., Ishii, K., Matsuura, Y., Miyamura, T., and Suzuki, T. (2001). Ubiquitin-mediated degradation of hepatitis C virus core protein is regulated by processing at its carboxyl terminus. *Virology* 280, 301–309.

Tanaka, T., Kato, N., Cho, M. J., and Shimotohno, K. (1995). A novel sequence found at the 3' terminus of hepatitis C virus genome. *Biochem. Biophys. Res. Commun.* 215, 744–749.

Targett-Adams, P., Hope, G., Boulant, S., and Mclauchlan, J. (2008). Maturation of hepatitis C virus core protein by signal peptide peptidase is required for virus production. *J. Biol. Chem.* 283, 16850–16859.

Tellinghuisen, T. L., Foss, K. L., and Treadaway, J. (2008). Regulation of hepatitis C virion production via phosphorylation of the NS5A protein. *PLoS Pathog.* 4, e1000032. doi:10.1371/journal.ppat.1000032

Tellinghuisen, T. L., Marcotrigiano, J., and Rice, C. M. (2005). Structure of the zinc-binding domain of an essential component of the hepatitis C virus replicase. *Nature* 435, 374–379.

Thomssen, R., Bonk, S., Propfe, C., Heermann, K. H., Kochel, H. G., and Uy, A. (1992). Association of hepatitis C virus in human sera with beta-lipoprotein. *Med. Microbiol. Immunol.* 181, 293–300.

Tsukiyama-Kohara, K., Iizuka, N., Kohara, M., and Nomoto, A. (1992). Internal ribosome entry site within hepatitis C virus RNA. *J. Virol.* 66, 1476–1483.

Vieyres, G., Thomas, X., Descamps, V., Duverlie, G., Patel, A. H., and Dubuisson, J. (2010). Characterization of the envelope glycoproteins associated with infectious hepatitis C virus. *J. Virol.* 84, 10159–10168.

Voisset, C., Lavie, M., Helle, F., Op De Beeck, A., Bilheu, A., Bertrand-Michel, J., Terce, F., Cocquerel, L., Wychowski, C., Vu-Dac, N., and Dubuisson, J. (2008). Ceramide enrichment of the plasma membrane induces CD81 internalization and inhibits hepatitis C virus entry. *Cell. Microbiol.* 10, 606–617.

Wakita, T., Pietschmann, T., Kato, T., Date, T., Miyamoto, M., Zhao, Z., Murthy, K., Habermann, A., Krausslich, H.-G., Mizokami, M., Bartenschlager, R., and Liang, T. J. (2005). Production of infectious hepatitis C virus in tissue culture from a cloned viral genome. *Nat. Med.* 11, 791–796.

Wang, C., Sarnow, P., and Siddiqui, A. (1993). Translation of human hepatitis C virus RNA in cultured cells is mediated by an internal ribosome-binding mechanism. *J. Virol.* 67, 3338–3344.

Wasley, A., and Alter, M. J. (2000). Epidemiology of hepatitis C: geographic differences and temporal trends. *Semin. Liver Dis.* 20, 1–16.

Wolk, B., Sansonno, D., Krausslich, H. G., Dammacco, F., Rice, C. M., Blum, H. E., and Moradpour, D. (2000). Subcellular localization, stability, and trans-cleavage competence of the hepatitis C virus NS3-NS4A complex expressed in tetracycline-regulated cell lines. *J. Virol.* 74, 2293–2304.

Wozniak, A. L., Griffin, S., Rowlands, D., Harris, M., Yi, M., Lemon, S. M., and Weinman, S. A. (2010). Intracellular proton conductance of the hepatitis C virus p7 protein and its contribution to infectious virus production. *PLoS Pathog.* 6, e1001087. doi:10.1371/journal.ppat.1001087

Yamamoto, M., Aizaki, H., Fukasawa, M., Teraoka, T., Miyamura, T., Wakita, T., and Suzuki, T. (2011). Structural requirements of virion-associated cholesterol for infectivity, buoyant density and apolipoprotein association of hepatitis C virus. *J. Gen. Virol.* 92, 2082–2087.

Yasui, K., Wakita, T., Tsukiyama-Kohara, K., Funahashi, S. I., Ichikawa, M., Kajita, T., Moradpour, D., Wands, J. R., and Kohara, M. (1998). The native form and maturation process of hepatitis C virus core protein. *J. Virol.* 72, 6048–6055.

Yi, M., and Lemon, S. M. (2003). 3' Nontranslated RNA signals required for replication of hepatitis C virus RNA. *J. Virol.* 77, 3557–3568.

Yi, M., Ma, Y., Yates, J., and Lemon, S. M. (2007). Compensatory mutations in E1, p7, NS2, and NS3 enhance yields of cell culture-infectious intergenotypic chimeric hepatitis C virus. *J. Virol.* 81, 629–638.

Yi, M., Ma, Y., Yates, J., and Lemon, S. M. (2009). Trans-complementation of an NS2 defect in a late step in hepatitis C virus (HCV) particle assembly and maturation. *PLoS Pathog.* 5, e1000403. doi:10.1371/journal.ppat.1000403

Zhong, J., Gastaminza, P., Cheng, G., Kapadia, S., Kato, T., Burton, D. R., Wieland, S. F., Uprichard, S. L., Wakita, T., and Chisari, F. V. (2005). Robust hepatitis C virus infection in vitro. *Proc. Natl. Acad. Sci. U.S.A.* 102, 9294–9299.

Conflict of Interest Statement: The author declares that the research was conducted in the absence of any commercial or financial relationships that could be construed as a potential conflict of interest.

Received: 16 December 2011; accepted: 23 January 2012; published online: 07 February 2012.

Citation: Suzuki T (2012) Morphogenesis of infectious hepatitis C virus particles. Front. Microbio. 3:38. doi: 10.3389/fmicb.2012.00038

This article was submitted to Frontiers in Virology, a specialty of Frontiers in Microbiology.

OPEN ACCESS Freely available online PLoS PATHOGENS

Visualization and Measurement of ATP Levels in Living Cells Replicating Hepatitis C Virus Genome RNA

Tomomi Ando[1,2], Hiromi Imamura[3], Ryosuke Suzuki[1], Hideki Aizaki[1], Toshiki Watanabe[2], Takaji Wakita[1], Tetsuro Suzuki[4]*

1 Department of Virology II, National Institute of Infectious Diseases, Tokyo, Japan, **2** Graduate School of Frontier Sciences, The University of Tokyo, Tokyo, Japan, **3** The Hakubi Center and Graduate School of Biostudies, Kyoto University, Kyoto, Japan, **4** Hamamatsu University School of Medicine, Department of Infectious Diseases, Hamamatsu, Japan

Abstract

Adenosine 5′-triphosphate (ATP) is the primary energy currency of all living organisms and participates in a variety of cellular processes. Although ATP requirements during viral lifecycles have been examined in a number of studies, a method by which ATP production can be monitored in real-time, and by which ATP can be quantified in individual cells and subcellular compartments, is lacking, thereby hindering studies aimed at elucidating the precise mechanisms by which viral replication energized by ATP is controlled. In this study, we investigated the fluctuation and distribution of ATP in cells during RNA replication of the hepatitis C virus (HCV), a member of the *Flaviviridae* family. We demonstrated that cells involved in viral RNA replication actively consumed ATP, thereby reducing cytoplasmic ATP levels. Subsequently, a method to measure ATP levels at putative subcellular sites of HCV RNA replication in living cells was developed by introducing a recently-established Förster resonance energy transfer (FRET)-based ATP indicator, called ATeam, into the NS5A coding region of the HCV replicon. Using this method, we were able to observe the formation of ATP-enriched dot-like structures, which co-localize with non-structural viral proteins, within the cytoplasm of HCV-replicating cells but not in non-replicating cells. The obtained FRET signals allowed us to estimate ATP concentrations within HCV replicating cells as ~5 mM at possible replicating sites and ~1 mM at peripheral sites that did not appear to be involved in HCV replication. In contrast, cytoplasmic ATP levels in non-replicating Huh-7 cells were estimated as ~2 mM. To our knowledge, this is the first study to demonstrate changes in ATP concentration within cells during replication of the HCV genome and increased ATP levels at distinct sites within replicating cells. ATeam may be a powerful tool for the study of energy metabolism during replication of the viral genome.

Citation: Ando T, Imamura H, Suzuki R, Aizaki H, Watanabe T, et al. (2012) Visualization and Measurement of ATP Levels in Living Cells Replicating Hepatitis C Virus Genome RNA. PLoS Pathog 8(3): e1002561. doi:10.1371/journal.ppat.1002561

Editor: Andrea Gamarnik, Fundación Instituto Leloir-CONICET, Argentina

Received August 22, 2011; **Accepted** January 18, 2012; **Published** March 1, 2012

Funding: This work was supported by a grant-in-aid for Scientific Research from the Japan Society for the Promotion of Science, from the Ministry of Health, Labour and Welfare of Japan and from the Ministry of Education, Culture, Sports, Science and Technology of Japan. T.A. is a research fellow of the Japan Society for the Promotion of Science. The funders had no role in study design, data collection and analysis, decision to publish, or preparation of the manuscript.

Competing Interests: The authors have declared that no competing interests exist.

* E-mail: tesuzuki@hama-med.ac.jp

Introduction

Adenosine 5′-triphosphate (ATP) is the major energy currency of cells and is involved in a variety of cellular processes, including the virus life cycle, in which ATP-dependent reactions essential for virus multiplication are catalyzed by viral-encoded enzymes or complexes consisting of viral and host-cell proteins [1]. However, the lack of a real-time monitoring system for ATP has hindered studies aimed at elucidating the mechanisms by which cellular processes are controlled through ATP. A method for measuring ATP levels in individual living cells has recently been developed using a genetically-encoded FRET-based indicator for ATP, called ATeam, which employs the epsilon subunit of a bacterial F_0F_1-ATPase [2]. The epsilon subunit has several theoretical advantages for use as an ATP indicator; i) small size (14 kDa), ii) high specific binding to ATP, iii) ATP binding induces a global conformational change and iv) ATP hydrolysis does not occur following binding [3–5]. The affinity of ATeam for ATP can be adjusted by changing various amino acid residues in the ATP-binding domain within the subunit. ATeam has enabled researchers to examine the subcellular compartmentation of ATP as well as time-dependent changes in cellular ATP levels under various physiological conditions. For example, the ATeam-based method has been used to demonstrate that ATP levels within the mitochondrial matrix are lower than those in the cytoplasm and the nucleus [2].

Hepatitis C virus (HCV) infects 2–3% of the world population and is a major cause of chronic hepatitis, liver cirrhosis and hepatocellular carcinoma [6–8]. HCV possesses a positive-strand RNA genome and belongs to the family *Flaviviridae*. A precursor polyprotein of ~3000 amino acids is post- or co-translationally processed by both viral and host proteases into at least ten viral products. The nonstructural (NS) proteins NS3, NS4A, NS4B, NS5A and NS5B are necessary and sufficient for autonomous HCV RNA replication. These proteins form a membrane-associated replication complex (RC), in which NS5B is the RNA-dependent RNA polymerase (RdRp) responsible for copying the RNA genome of the virus during replication [9,10]. NS3, in addition to its protease activity, functions as a viral helicase capable of separating duplex RNA and DNA in reactions fuelled

Author Summary

ATP is the major energy currency of living cells. Replication of the virus genome is a physiological mechanism that is known to require energy for operations such as the synthesis of DNA or RNA and their unwinding. However, it has been difficult to comprehend how the ATP level is regulated inside single living cells where the virus replicates, since average ATP values in cell extracts have only been estimated using existing methods for ATP measurement. ATeam, which was established in 2009, is a genetically-encoded Förster resonance energy transfer (FRET)-based indicator for ATP that is composed of a small bacterial protein that specifically binds ATP sandwiched between two fluorescent proteins. In this study, by applying ATeam to the subgenomic replicon system, we have developed a method to monitor ATP at putative subcellular sites of RNA replication of the hepatitis C virus (HCV), a major human pathogen associated with liver disease, in living cells. We show here, for the first time, changes in ATP concentrations at distinct sites within cells undergoing HCV RNA replication. ATeam might open the door to understanding how regulation of ATP can affect the lifecycles of pathogens.

by ATP hydrolysis [11,12]. Consistent with other positive-strand RNA viruses, replication of HCV genomic RNA is believed to occur in membrane-bound vesicles. NS3-NS5B proteins, together with several host-cell proteins, form a membrane-associated RC. The HCV RC is localized to distinct dot-like structures within the cytoplasm of HCV replicating cells and can be detected in detergent-resistant membrane structures [13].

In this study, we first used capillary electrophoresis-time-of-flight mass spectrometry (CE-TOF MS) and the original ATeam method to determine ATP levels in cells infected with HCV or replicating HCV RNA. Using these methods, together with an ATP consumption assay, we demonstrated that ATP is actively consumed in cells in which viral RNA replicates, leading to a reduction in cytoplasmic ATP compared to parental cells. To further understand the fluctuation and distribution of ATP in HCV replicating cells, we developed a system to monitor ATP at putative subcellular sites of HCV RNA replication in single living cells by applying ATeam technology to the subgenomic replicon system. Our results show that, in viral RNA-replicating cells, ATP levels are elevated at distinct dot-like structures that may play a supportive role in HCV RNA replication, while cytoplasmic levels of ATP decrease.

Results

The concentration of ATP is reduced in HCV-infected cells

As a first approach, the concentration of adenosine nucleotides within HCV-infected and non-infected cells was quantified by CE-TOF MS analysis. ATP levels were approximately 7- and 50-fold higher, respectively, than the levels of ADP and AMP in non-infected Huh-7 cells (Figure 1A). At 9 days post-infection with HCV particles produced from a wild-type JFH-1 isolate [14], the intracellular levels of ATP, ADP and AMP were significantly (52–59%) lower than those in naïve Huh-7 cells (Figure 1A). ATP/ADP and ATP/AMP ratios were comparable among HCV-infected and non-infected cells (Figure 1B). A similar result was obtained using JFH-1/4-5 cells that harbor a HCV subgenomic replicon (SGR) RNA derived from the JFH-1 isolate [15]; the intracellular ATP level of JFH-1/4-5 cells was lower than that of parental Huh-7 cells (Figure S1). These findings are basically consistent with a recent report that phosphorylation-mediated activation of AMP-activated protein kinase is inhibited in cells undergoing HCV genome replication, and that ATP/ADP ratios are similar among cells that do and do not demonstrate HCV replication [16,17].

Measurement of ATP levels in HCV-replicating cells using ATeam

To visualize ATP levels in living cells undergoing HCV genomic replication, one of the ATeam indicators, AT1.03^{YEMK}, which has a high affinity for ATP, was introduced into HCV replicon cells carrying SGR RNA or into parental Huh-7 cells and was imaged using confocal fluorescence microscopy. Consistent with previous observations in HeLa cells [2], this ATP indicator was distributed throughout the cytoplasm. FRET signals (Venus/

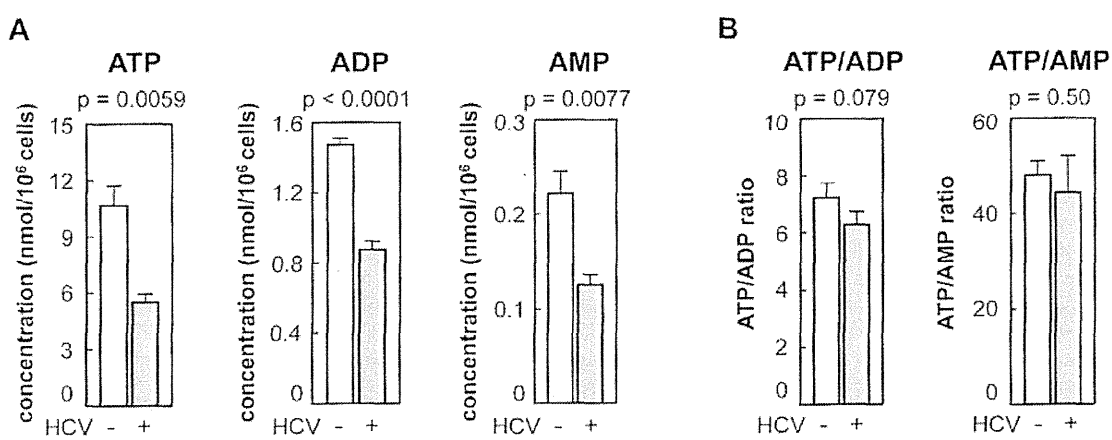

Figure 1. Levels of adenosine nucleotides in HCV-infected and non-infected Huh-7 cells determined by CE-TOF MS. (A) ATP levels were reduced in HCV-infected cells. ATP, ADP, and AMP metabolites in Huh-7 cells with (gray bars) and without (open bars) HCV infection were measured by CE-TOFMS. (B) Ratios of ATP/ADP and ATP/AMP were calculated from the results depicted in (A). All data are presented as means and standard deviation (SD) values for three independent samples. Statistical differences between HCV-infected and non-infected cells were evaluated using Student's *t*-test.
doi:10.1371/journal.ppat.1002561.g001

CFP fluorescence emission ratios), which reflect ATP levels in living cells, were calculated from the fluorescent images of CFP and Venus, a variant of YFP that is resistant to intracellular pH [18], within the cytoplasm of individual cells. Each independent measurement was plotted as indicated in Figure 2. Uniform Venus/CFP ratios were observed in Huh-7 cells. These ratios were reduced dramatically following combined treatment with 2-deoxyglucose (2DG) and Oligomycin A (OliA), which inhibit glycolysis and the oxidative phosphorylation of ADP to ATP, respectively [2]. When AT1.03^{YEMK} was expressed in the HCV replicon-harboring cells JFH-1/4-1, JFH-1/4-5 (genotype 2a) and NK5.1/0-9 (genotype 1b) [15], Venus/CFP ratios were significantly lower than those seen in parental Huh-7 cells. This result is consistent with the mass spectrometry results shown in Figures 1A and S1. Venus/CFP ratios were more variable in the replicon-carrying cells compared to Huh-7 cells. It is possible that ATP levels in the replicon cells correlate with viral replication levels, which may vary among the cells tested.

The consumption of ATP is increased in HCV-replicating cells

It has been reported that ATP is involved in different steps in the course of HCV replication such as in the initiation of RNA synthesis by NS5B RdRp [9]. NS3 unwinds RNA in an ATP-dependent manner and may be involved in viral replication [11,19,20]. NS4A has been shown to enhance the ability of the NS3 helicase to bind RNA in the presence of ATP [21]. In addition, ATP is generally used as a material in RNA synthesis. Together with the above results (Figures 1 and 2), one may hypothesize that active consumption of ATP in cells where HCV RNA replicates efficiently results in lower levels of cytoplasmic ATP compared to cells in the absence of the viral RNA. To study the influence of HCV RNA replication on the consumption of ATP in cells, we used permeabilized HCV replicon cells [13,22].

Following the addition of ATP to permeabilized cells, reduced ATP levels were detected using a luciferase-based assay (see Materials and Methods for details). Fifteen minutes after the addition of ATP, ATP levels in permeabilized replicon-carrying cells (JFH-1/4-1, JFH-1/4-5 and NK5.1/0-9) were reduced by 82–95%, and this reduction was greater than that observed in control Huh-7 cells (47%)(Figure 3). When the replication of HCV RNA was inhibited by pre-treatment of the cells with the cytidine analogue inhibitor of HCV NS5B polymerase, PSI-6130 [23,24], for 3 days, the reduction in ATP levels in the replicon cells was comparable to that of Huh-7 cells. A decrease in ATP reduction in the replicon cells was observed even following a 15-min treatment with the inhibitor. An effect of inhibition of viral replication on cytoplasmic ATP levels in replicon cells was also observed by ATeam-based analysis of Venus/CFP ratios following inhibition of replication by IFN-alpha (Figure S2). These results suggest that ATP is actively consumed during viral replication in HCV replicon cells, leading to decreased levels of ATP in the cytoplasm.

Development of a system to monitor ATP levels at putative subcellular sites of HCV replication in single living cells

Moradpour et al. have established functional HCV replicons that have either an epitope tag or the coding sequence for a green fluorescent protein (GFP) inserted in frame close to the C-terminus of NS5A, which they used to demonstrate incorporation of the NS5A-GFP fusion protein into the viral RC [25]. To further investigate intracellular changes in ATP during HCV replication, we generated HCV JFH-1-based subgenomic replicons harboring an ATeam insertion in the 3′ region of NS5A (SGR-ATeam), as

	No. cells	Venus/CFP ratio mean	Venus/CFP ratio SD	p-value vs Huh-7
Huh-7	19	2.08	0.090	
Huh-7 + 2DG, OliA	13	0.66	0.074	$< 1x10^{-29}$
JFH-1/4-1	18	1.79	0.14	$< 1x10^{-7}$
JFH-1/4-5	18	1.77	0.28	0.00019
NK5.1/0-9	19	1.66	0.30	$< 1x10^{-5}$

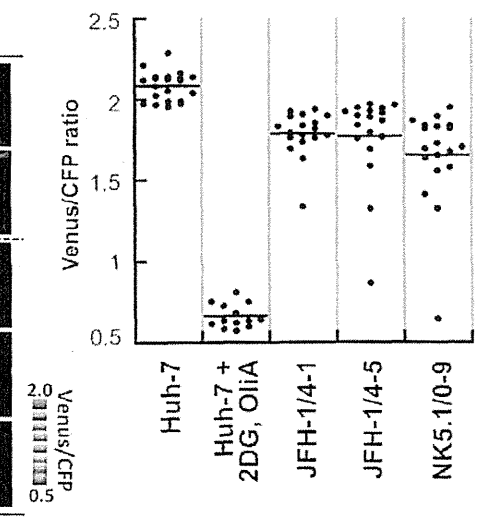

Figure 2. ATP fluctuations within the cytoplasm of HCV replicating cells analyzed using the original ATeam. Huh-7 cells carrying a HCV subgenomic replicon, JFH-1/4-1, JFH-1/4-5 (genotype 2a), and NK5.1/0-9 (genotype 1b) and parental Huh-7 cells were transfected with an ATP probe, AT1.03^{YEMK}. Forty-eight hours after transfection, the Venus/CFP emission ratio in the cytoplasm of each cell was calculated from fluorescent images acquired with a confocal microscope FV1000 (Olympus). Huh-7 cells treated with 10 mM 2-DG and 10 μg/ml OliA for 20 min were used as a negative control. Data are presented as means and standard deviation values (SD) for each cell. Statistical differences among Huh-7 cells were evaluated using Student's *t*-test. Pseudocolored images of Venus channel/CFP channel ratios of representative cells and a pseudocolor scale are shown. In the graph on the right, each plot indicates the Venus/CFP ratio of each cell. The horizontal lines in the center represent the mean values for each group.
doi:10.1371/journal.ppat.1002561.g002

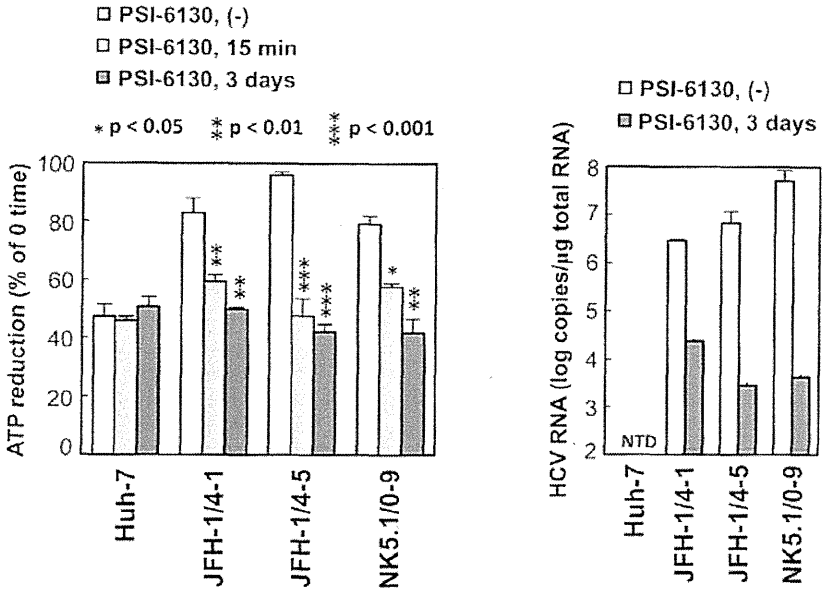

Figure 3. ATP consumption in cells replicating HCV RNA. (Left) The indicated cell lines were pretreated with 10 μM PSI-6130 for 3 days or were cultured in the absence of the drug, followed by trypsinization and permeabilization. ATP-containing reaction buffer plus 10 μM PSI-6130 was added to some of the non-pre-treated cells (PSI-6130, 15 min; light gray bars). ATP-containing PSI-6130-free reaction buffer was added to the rest of the non pre-treated cells (PSI-6130, (−); white bars) and to the pre-treated cells (PSI-6130, 3 days; dark gray bars). After 15 min incubation, ATP levels in cell lysates were measured using a luciferase-based assay. ATP reduction compared to ATP levels at the 0-time point was calculated. The mean values of three independent samples with SD are displayed. Statistical differences between cells treated with and without treatment with PSI-6130 were evaluated using Student's *t*-test. (Right) HCV RNA titers in cells corresponding to the left panel were determined using real-time quantitative RT-PCR. Data are presented as means and SD for three independent samples. NTD indicates not detected.
doi:10.1371/journal.ppat.1002561.g003

well as plasmids expressing NS5A-ATeam fusion proteins (NS5A-ATeam)(Figures 4A and 4C).

We first tested whether NS5A-ATeam fusion proteins can be used to monitor ATP levels over a range of concentrations in living cells. The Venus/CFP ratios in individual cells expressing NS5A fused either with AT1.03^{YEMK} (Kd = 1.2 mM at 37°C [2]) or with a relatively lower affinity version, AT1.03 (Kd = 3.3 mM at 37°C [2]) were measured. As shown in Figure 4B, differences in the Venus/CFP ratios of NS5A- AT1.03^{YEMK} and NS5A-AT1.03 were similar to those of AT1.03^{YEMK} and AT1.03, although average ratios were lower for NS5A- AT1.03^{YEMK} and NS5A-AT1.03 compared to AT1.03^{YEMK} and AT1.03. In the presence of 2DG and OliA, Venus/CFP ratios of NS5A-AT1.03^{YEMK} were markedly reduced to levels that were comparable to those of AT1.03^{RK}, an inactive mutant with R122K/R126K substitutions [2]. These results demonstrate that NS5A-ATeams can function as ATP indicators, although their dynamic ranges of Venus/CFP ratios are slightly smaller than those of the original, non-fused ATeams.

We next investigated whether the SGR-ATeam could initiate and sustain transient replication of HCV RNA in cells. A RNA polymerase I (Pol I)-derived plasmid, which carries SGR/luc-AT1.03 containing a luciferase reporter gene ([26]; Figure 4C), or its replication-defective mutant were transfected into Huh-7 cells and levels of viral replication were determined by measuring luciferase activity at various time intervals over a five day period (Figure 4D). Although replication of SGR/luc-AT1.03 was delayed compared with parental SGR/luc, the luciferase activity expressed from SGR/luc-AT1.03 rose to approximately a thousand-fold higher than that expressed from SGR/luc-GND-AT1.03 at five days post-transfection. It appears that SGR-AT1.03, which does not carry the luciferase gene, replicated more efficiently than SGR/luc-AT1.03, as determined by Western blotting of the HCV NS5B protein within cells four days post-transfection (Figure 4E). As indicated in Figure 4F, an abundant protein of the same size as that expected for the NS5A-ATeam fusion protein was observed in cells expressing either NS5A-AT1.03 or SGR-AT1.03, indicating that the NS5A-ATeam fusion protein is stable and is not cleaved during HCV replication. Thus, we concluded that the modified replicon constructs in which the ATeam is incorporated into the NS5A region are functional and remain capable of efficient transient replication of HCV RNA.

Visualization of ATP levels and distinctive features of ATP distribution in cells replicating ATeam-tagged SGR

This SGR-ATeam system that was established to analyze cellular ATP levels was used in living HCV RNA-replicating cells in which membrane-associated RCs are formed through the interaction of viral proteins, including NS5A, and cellular proteins. We compared the subcellular distribution of fluorescent signals expressed from NS5A-ATeams and SGR-ATeams using emission-scanning confocal fluorescence microscopy with a Zeiss META detector. NS5A-AT1.03 and NS5A-AT1.03^{YEMK} were diffusely distributed throughout the cytoplasm (Figure 5A; upper panels). Venus/CFP ratios of NS5A-ATeam constructs were almost constant throughout the cytoplasm (Figure 5A; lower). As expected, Venus/CFP ratios in cells expressing NS5A-AT1.03^{YEMK} were markedly higher than those of NS5A-AT1.03 (Figure 5A; lower). In contrast, cells replicating SGR-AT1.03 and SGR-AT1.03^{YEMK} showed foci of brightly fluorescent dot-like structures in the cytoplasm (Figure 5B; upper panels). Interestingly, some of these fluorescent foci had an apparently higher Venus/

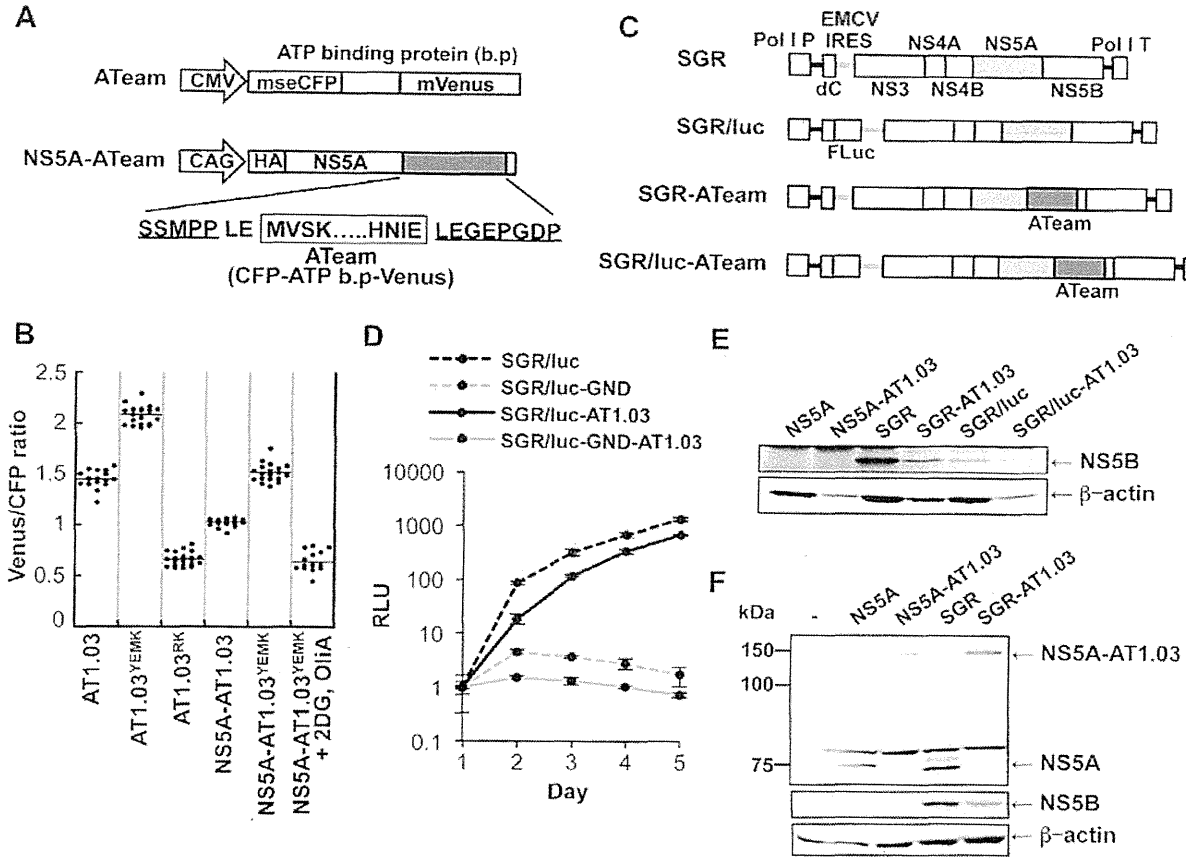

Figure 4. Development of NS5A-ATeam and SGR-ATeam to enable real-time monitoring of ATP. (A) Schematic representation of the ATeam and NS5A-ATeam used in this study. ATeam genes were inserted into the 3′ region of a HA-NS5A expression vector to generate NS5A-ATeam. The underlined sequences indicate NS5A residues. The insertion site was between residues 2394 and 2395, numbered according to the polyprotein of the HCV JFH-1 isolate. CMV, Cytomegalovirus promoter; CAG, CAG promoter; ATP b.p, ATP binding protein. HA, HA tag. (B) Huh-7 cells were transfected with ATeam and NS5A-ATeam constructs. Forty-eight hours post-transfection, the Venus/CFP ratios of each cell were calculated from fluorescent images acquired with a confocal microscope in the same way as described in the legends for Figure 2. Each plot shows the ratio of individual cells. Horizontal lines represent means. (C) Schematic representation of the SGR and SGR-ATeam plasmids used, with or without the firefly luciferase gene (Fluc). HCV polyproteins are indicated by the open boxes. ATeam genes were inserted into the same site in the NS5A C-terminal region. Bold lines indicate the HCV UTR. EMCV IRES is denoted by the gray bars. Pol I P, Pol I promotor; dC, 5′ region of Core gene; Pol I T, Pol I terminator. (D) Replication levels of SGR/luc-AT1.03 in transfected cells were determined by luciferase assay 1–5 days post-transfection. SGR/luc and SGR/luc-GND were used as positive and negative controls, respectively. Values given were normalized for transfection efficiency with luciferase activity determined 24 h post-transfection. All data are presented as means and SD for three independent samples. (E) Huh-7 cells were transfected with constructs encoding NS5A, NS5A-AT1.03, SGR, SGR-AT1.03, SGR/luc or SGR/luc-AT1.03, followed by immunoblotting with anti-NS5B or anti-beta-actin antibody. (F) Cells transfected with constructs encoding NS5A, NS5A-AT1.03, SGR or SGR-AT1.03 were analyzed by immunoblotting with anti-NS5A, anti-NS5B or anti-beta-actin antibodies.
doi:10.1371/journal.ppat.1002561.g004

CFP ratio than the surrounding cytoplasmic region (Figure 5B; middle and lower panels). Although the number of high Venus/CFP ratios was not consistent between the cells, this phenotype was observed in most of the cells that were replicating SGR-AT1.03 (Figure S3). Such high focal Venus/CFP ratios were not detected in cells replicating SGR-AT1.03^{RK} or in SGR-AT1.03^{YEMK} -replicating cells treated with 2DG and OliA. Thus, foci with a high Venus/CFP ratio apparently represent the presence of high ATP levels at distinct sites in cells replicating HCV RNA. In addition, when a replication-defective polyprotein that extended from NS3 through to the NS5B protein, including NS5A-AT1.03, was expressed, no high Venus/CFP ratio was seen in the cells in spite of the fact that NS5A-AT1.03 was detected in dot-like structures throughout the cytoplasm (Figure S4). These results strongly suggest that the high Venus/CFP ratios observed using the SGR-ATeam system are associated with the replication of HCV RNA.

To investigate whether the high Venus/CFP ratios of the dot-like structures detected in cells replicating SGR-ATeam are located at the HCV RC, FRET images of SGR-AT1.03-replicating cells were analyzed, followed immunofluorescence analysis of cells fixed and stained with either anti-NS5A or anti-NS3 antibodies (Figure 5C). Confocal fluorescence microscopy at high magnification demonstrated that the high Venus/CFP ratios that were identified in foci of various sizes were co-localized with NS5A and NS3 that were possibly membrane-bound within the cytoplasm of the viral replicating cells. Some of the NS3- or NS5A-labeled proteins that were identified by immunofluorescence were not associated with high Venus/CFP ratios. These results are consistent with previous reports, which demonstrated that only

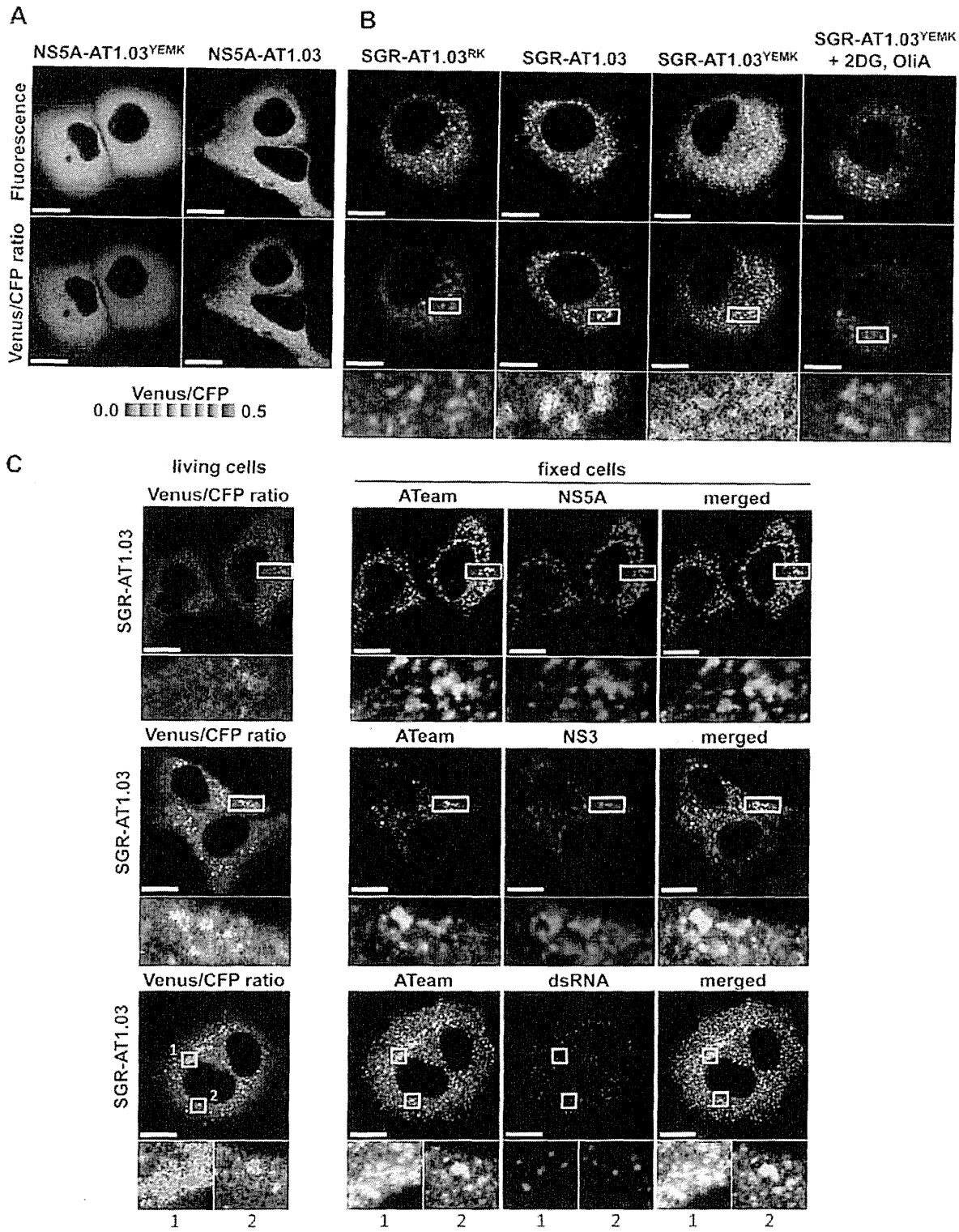

Figure 5. Visualization of sites of focal accumulation of ATP in cells expressing NS5A-ATeam or SGR-ATeam. (A) Huh-7 cells were transfected with NS5A-AT1.03 or NS5A-AT1.03^{YEMK}. Four days after transfection, the cells were analyzed using spectral imaging (405-nm excitation) of LSM510-META (Carl Zeiss). Images were processed to the CFP channel (F_{CFP}) and the Venus channel (F_{Venus}) using a linear unmixing algorithm using a reference for each spectrum. The upper panels demonstrate the signal intensity from a spectral channel with maximum intensity and represent the expression pattern of NS5A-ATeam. The lower panels are constructed from FRET ratio images (F_{CFP}/F_{Venus}) with pseudocolors. The pseudocolor scale is shown below. Scale bars, 20 μm. (B) Huh-7 cells were transfected with SGR-AT1.03^{RK}, SGR-AT1.03 or SGR-AT1.03^{YEMK}, and were analyzed in the same

way as described in (A). SGR-AT1.03^{YEMK} -transfected cells were treated with 10 mM 2DG and 10 μg/ml OliA just before imaging and were used as a negative control. The upper panels demonstrate the intensity from a spectral channel with maximum intensity and represent the expression pattern of NS5A-ATeam processed from SGR-ATeam. The lower panels indicate square areas within FRET ratio panels magnified five-fold. Scale bars, 20 μm. (C) Cells were fixed after live-cell FRET imaging, and the same cell was analyzed by indirect immunofluorescence staining. Viral proteins were labeled with antibodies against NS5A (upper panels), NS3 (middle panels) and dsRNA (lower panels), which were detected with an Alexa Fluor 555-labeled anti-rabbit or anti-mouse antibody. ATeam panels (green) represent the expression of NS5A-ATeam processed from SGR-ATeam, and NS5A, NS3 or dsRNA panels (red) represent the immunostained signals. Enlarged views of the areas outlined by squares at a five-fold magnification are also shown. Scale bars, 20 μm.
doi:10.1371/journal.ppat.1002561.g005

some of the expressed HCV NS proteins contribute to viral RNA synthesis [27]. To further investigate the relationship between the cellular sites at which there was a high Venus/CFP ratio and HCV RNA replication, double-stranded RNA (dsRNA) was visualized by staining with a specific anti-dsRNA antibody after FRET imaging (Figure 5C). This staining indicated that dsRNA-containing dot-like structures co-localized with structures that displayed high Venus/CFP ratios. Therefore, it is most likely that the dot-like structures with high Venus/CFP ratios that were detected using the SGR-ATeam system reflect the sites of HCV RNA replication or HCV RCs.

Several studies have shown that mitochondria, which play a central role in ATP metabolism, localize to areas near the membranous web, the likely site of HCV RNA replication [28]. We thus compared the subcellular localization of the fluorescence signals detected in cells expressing SGR-ATeam with that of mitochondria that were visualized by staining with Mitotracker. Foci with high Venus/CFP ratios did not colocalize with, but were localized adjacent to mitochondria in cells that were replicating SGR-AT1.03 (Figure S5). This finding might reflect the fact that ATP can be directly supplied from mitochondria to the sites of viral RNA replication in cells.

Quantification of ATP at putative cytoplasmic sites of HCV RNA replication within cells

Based on the above observations, FRET signals detected within cells expressing SGR-ATeam or NS5A-ATeam can be classified as either signals from distinct dot-like structures, which represent putative subcellular sites of HCV RNA replication, or as signals that are diffuse throughout the cytoplasm. The Venus/CFP emission ratio in individual cells into which NS5A-AT1.03, NS5A-AT1.03^{YEMK}, SGR-AT1.03, SGR-AT1.03^{YEMK} or SGR-AT1.03^{RK} was introduced was determined (Figure 6A). Fluorescent signals corresponding to cytoplasmic ATP were identified by subtracting signals at putative sites of viral RNA replication from signals from the cytoplasmic area as a whole. Cytoplasmic Venus/CFP ratios within cells replicating SGR-AT1.03 and SGR-AT1.03^{YEMK} were lower than those in cells expressing NS5A-AT1.03 and NS5A-AT1.03^{YEMK}, respectively. Therefore, cytoplasmic ATP levels within HCV RNA-replicating cells were lower than in non-replicating cells. This result is consistent with the findings shown in Figure 1A. The average Venus/CFP ratios at potential sites of viral RNA replication were greater than the corresponding cytoplasmic levels in cells replicating SGR-AT1.03 or SGR-AT1.03^{YEMK}. As expected, a significant decrease in Venus/CFP ratios was observed in cells treated with 2DG and OliA.

We next quantified ATP levels within individual cells replicating HCV RNA based on the Venus/CFP ratios obtained. To generate standard curves for this calculation, permeabilized cells expressing NS5A-AT1.03 or NS5A-AT1.03^{YEMK} were prepared by digitonin treatment, followed by the addition of defined concentrations of ATP and subsequent FRET analysis [29,30]. As shown in Figure 6B, under these experimental conditions, baseline Venus/CFP ratios of approximately 0.1 were detected in the absence of exogenous ATP, and Venus/CFP ratios were observed to increase linearly with increasing ATP concentration. The standard curves thus obtained can be used to estimate the ATP concentrations of unknown samples in which a particular ATeam containing an ATP probe at the C terminus of HCV NS5A, such as NS5A-ATeam or SGR-ATeam, have been introduced. Based on the fluorescent signal obtained in cells replicating SGR-ATeam, as well as in cells expressing NS5A-ATeam, the ATP concentration at putative sites of HCV RNA replication was estimated to be ~3 mM in the experiments shown in Figures 5A and 5B (average value of putative replication sites; 4.8 mM). After subtraction of the ATP that was localized at the HCV replication sites, the ATP concentration of HCV-replicating SGR cells (~1 mM) was found to be approximately half that observed in parental non-replicating cells (~2 mM)(average values in SGR and parental cells; 0.8 mM and 2.2 mM, respectively). To our knowledge, this is the first experiment in which ATP levels were estimated inside living cells during viral genome replication.

Figures 5 and 6A demonstrate changes in ATP concentrations at distinct sites in cells undergoing HCV RNA replication. Finally, we determined the effect of the PSI-6130 inhibitor of HCV replication on the change in subcellular ATP concentration in cells following introduction of SGR-AT1.03, SGR-AT1.03^{RK} or NS5A-AT1.03 (Figure 6C). In general, nucleoside analogue inhibitors of viral replication prevent RNA/DNA synthesis by chain termination immediately after addition to infected cells [23]. Indeed, as shown in Figure 3, a decrease in ATP consumption was detected even following a PSI-6130 treatment period as short as 15 min of permeabilized HCV replicon cells. We therefore analyzed and estimated ATP levels in cells in the presence of PSI-6130 for 10 min and 2 h. ATP concentrations at putative sites of viral RNA replication, as well as cytoplasmic ATP levels, were higher in SGR-AT1.03-replicating cells in the presence of 0.1–5 μM PSI-6130 for 10 min compared to the same cells without inhibitor treatment or to NS5A-AT1.03-expressing cells. A dose-dependent PSI-6130-induced increase in ATP levels at the putative replication sites was observed under the condition used. By treatment with PSI-6130 for 2 h, the ATP levels at putative replication sites were significantly lower than those without inhibitor treatment in SGR-AT1.03-replicating cells. The cytoplasmic ATP levels were similar with or without 2-h treatment (Figure 6C). In HCV SGR-ATeam cells treated with PSI-6130 for 3 days, HCV RNA replication was dramatically inhibited by greater than 90% with no observed cytotoxicity (Figure S6) and, as expected, little or no high Venus/CFP signal was detected anywhere in the cells (data not shown). We adapted the ATeam system to monitor ATP in HCV RNA replicating cells and found increased ATP levels at the putative subcellular sites of the viral replication. Findings obtained from experiments using the viral polymerase inhibitor strongly suggest that changes in ATP concentrations at the distinct sites observed depend on the viral RNA replication.

Discussion

This paper is the first to demonstrate changes in ATP within cells during viral genome replication. ATP requirements during

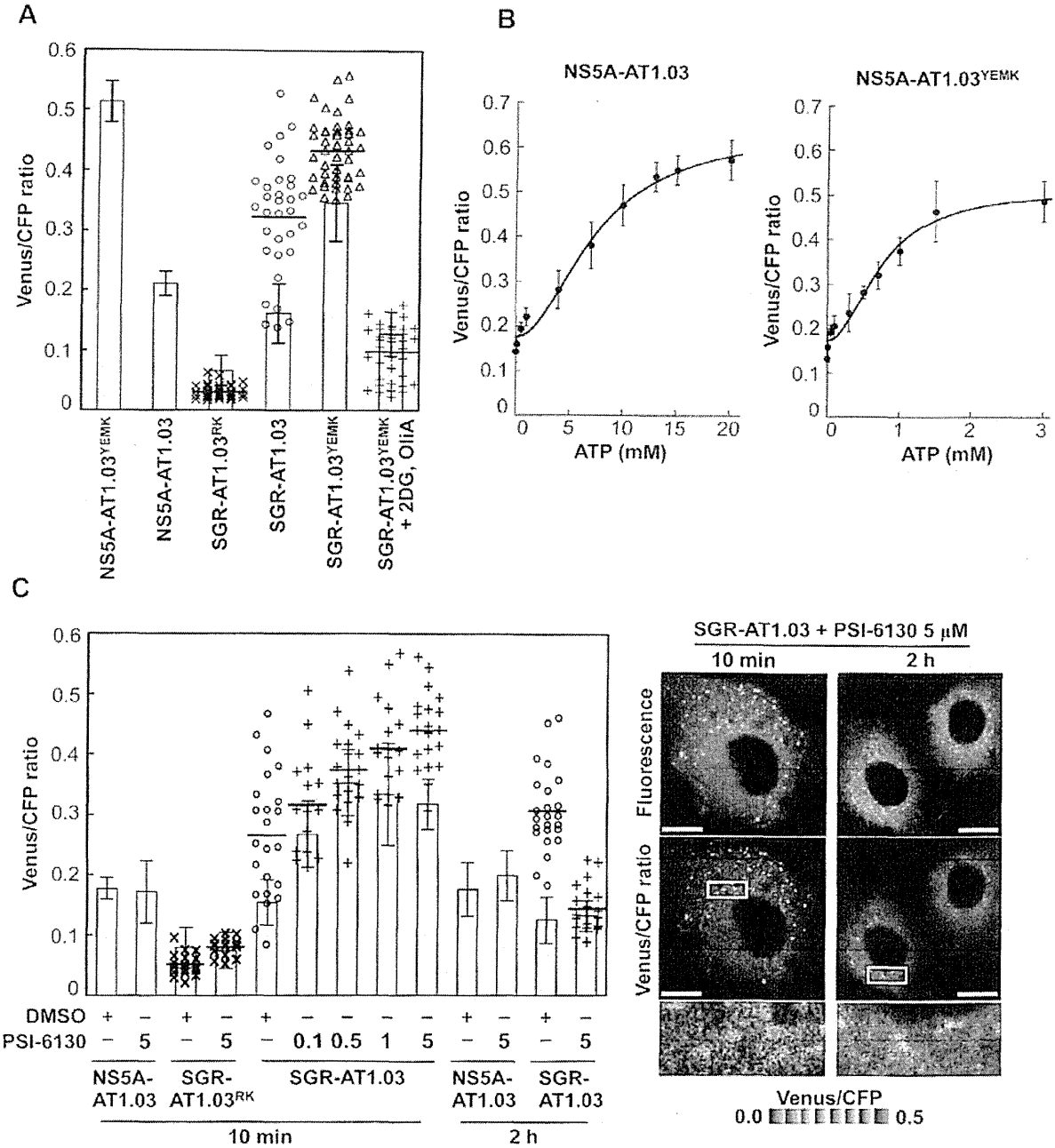

Figure 6. Estimation of ATP levels at possible sites of HCV RNA replication in living cells. (A) Venus/CFP emission ratios were calculated from images of CFP and Venus channels in individual cells for each group. Bar- and dotted graphs indicate ratios within the cytoplasm and ratios for dot-like structures, respectively, in the same cells, as shown in Figures 5A and 5B. Data in bar graphs are indicated as means and SD. Horizontal lines in the dot graphs denote means from at least three independent cells. Values in the cytoplasm of cells transfected with NS5A-AT1.03^{YEMK} and SGR-AT1.03^{YEMK} were statistically significant ($p<0.05$) as evaluated using the Student's *t*-test. (B) Calibration of NS5A-ATeam in cells under semi-intact conditions. Cells were transfected with NS5A-AT1.03 and NS5A-AT1.03^{YEMK}, respectively. Forty-eight hours later, the cells were permeabilized, followed by addition of known concentrations of ATP. FRET analyses were performed as described in Figure 5A. Each trace represents mean with SD of at least six independent cells. Plots were fitted with Hill equations with a fixed Hill coefficient of 2; $R=(R_{max}-R_{min})\times[ATP]^2/([ATP]^2+Kd^2)+R_{min}$, where R_{max} and R_{min} are the maximum and minimum fluorescence ratios, respectively. *Kd* is the apparent dissociation constant. R values were 0.994 and 0.986 for NS5A-AT1.03 and NS5A-AT1.03^{YEMK}, respectively. (C) Cells were transfected with NS5A-AT1.03, SGR-AT1.03^{RK} or SGR-AT1.03. The cells were then treated with PSI-6130 at indicated concentrations (μM) for 10 min or 2 h, and were analyzed as described in (A). Values in the cytoplasm of cells transfected with SGR-AT1.03 with and without PSI-6130 treatment were statistically significant ($p<0.05$ for control versus 0.1 or 1 μM PSI-6130, $p<0.01$ for control versus 0.5 or 5 μM PSI-6130) as evaluated using the Student's *t*-test. Representative cells treated with 5 μM PSI-6130 are shown in the right panel. The lower panel is a five-fold magnification of the boxed area. Scale bars, 20 μm.
doi:10.1371/journal.ppat.1002561.g006

the virus lifecycle have been studied for years. Several key steps during the viral life cycle, such as genome synthesis, require high-energy phosphoryl groups. For instance, it has been shown that ATP is required for the formation of a preinitiation complex for de novo RNA synthesis by RdRp of flaviviruses [31]. Transcriptional initiation and RNA replication by influenza virus RdRp are functional in an ATP-dependent fashion [32,33]. An ATP requirement of viral helicase activities has also been reported [34]. Furthermore, it has been demonstrated that ATP is involved in the assembly and/or release of viral structural proteins possibly via interaction with ATP-dependent chaperones [35,36]. However, it has been controversial as to whether ATP can be concentrated in particular subcellular compartment(s) in infected cells during viral replication. One of the underlying reasons for this controversy may be that a method by which cellular ATP levels can be determined, apart from examination of ATP levels in cellular extracts in the steady-state, has been lacking [37]. Recently Imamura et al. established FRET-based indicators, known as ATeams, for ATP quantification, and have shown that the use of ATeams enables the monitoring of ATP levels in real-time in different cellular compartments within individual cells [2].

In this study, in order to visualize and monitor ATP levels in living cells during replication of the viral genome, we first introduced the original ATeam-expressing plasmids into cells and found that cytoplasmic ATP levels in cells undergoing HCV genotype 1b and 2a RNA replication were lower than those in cured or parental cell lines (Figures 2 and S2). These results agree with the results of CE-TOF MS analysis (Figure 1) and the ATP consumption assay (Figure 3). It is therefore likely that ATP is actively consumed in cells during viral RNA replication, resulting in reduced levels of ATP in the cytoplasm. Furthermore, NS5A-ATeam fusion constructs, in which the ATeam gene was introduced into the C-terminal end of the NS5A coding region, and SGR-ATeam constructs containing a HCV JFH-1-derived subgenomic replicon within the NS5A-ATeam fused sequence as described above, were engineered (Figure 4). The results obtained using several ATeam fusion constructs with different affinities for ATP indicated that NS5A-ATeam fusion constructs can be used as FRET-based ATP indicators, and that the ATeam-tagged HCV replicons are capable of transient replication of viral RNA (Figure 4). It is interesting that our experiment using a SGR-ATeam construct provides evidence for the formation of ATP-enriched foci within cells that support HCV RNA replication (Figures 5 and 6). FRET-signal detection followed by indirect immunofluorescence allowed us to visualize co-localization of viral proteins as well as dsRNA at sites of ATP accumulation in cells (Figure 5), suggesting that these membrane-associated ATP-enriched foci likely represent sites of HCV RNA replication in transient replication assays.

Attempting to precisely quantify ATP within individual cells or particular intracellular compartments is a very challenging process. The luciferin-luciferase reaction has been utilized to monitor cellular ATP levels by measuring the released photon count during catalysis of bioluminescent oxidation by firefly luciferase. A previous study based on the luciferin-luciferase assay estimated basal cytoplasmic ATP levels at ~1.3 mM, which increased to ~5 mM during apoptotic cell death [38]. However, the results obtained were likely influenced by cellular levels of luciferase and other assay components, as well as by the pH of the cells. In this study, we describe quantification of ATP in human hepatoma Huh-7 cells undergoing HCV RNA replication using SGR-ATeam technology. Although ATP requirements during the lifecycles of various viruses have been studied for years, the use of ATeam technology enabled us, for the first time, to evaluate ATP concentrations at sites of viral replication within living cells. We here demonstrate that ATP concentrations at these putative subcellular sites of HCV RNA replication approach ~5 mM (Figure 6). This ATP level is as high as that observed during apoptotic processes such as caspase activation and DNA fragmentation, even though the latter ATP level was determined using a different assay system [38]. Considering that these apoptotic events were not observed at basal ATP levels [38], replication of the viral genome likely also requires high concentrations of cellular ATP. It should be noted that, in contrast to the fluorescent reporter system traditionally used to calculate the ATP/ADP ratio [39], the bacterial epsilon subunit used in ATeam is highly specific for ATP, but not for other nucleotides such as ADP, CTP, GTP or UTP [2,3]. In evaluating the effect of the HCV polymerase inhibitor on changes in the subcellular ATP concentration in cells replicating SGR-ATeam, an increase in ATP concentration was observed both at putative replication sites and in the cytoplasm of SGR-AT1.03-replicating cells in the presence of PSI-6130 for 10 min (Figure 6C). By contrast, 2-h treatment with the inhibitor resulted in reduction of ATP levels at putative replication sites in the replicon cells. Although the result of the experiment with 10-min treatment may be somewhat unexpected, it might possibly be explained by the following hypothesis. PSI-6130 began to inhibit viral RNA synthesis, leading to a decrease in ATP consumption. Since a mechanism for ATP transport mediated by host cell and/or viral factor(s) is still active during this time period, the ATP level at the replication sites should be increased compared to that during active replication. Higher levels of metabolic intermediates for glyconeogenesis as well as for glycolysis in HCV-infected cells compared to non-infected cells as determined via metabolome analysis (data not shown) may also be implicated in the increased ATP levels at the initial stage of inhibition of HCV replication. It is likely that active consumption of ATP caused by HCV replication and ATP transportation into the replication sites would lead to reduction of cytoplasmic ATP level. Such a change in ATP balance may result in induction of ATP generation and increase in certain metabolic intermediates related to glucose metabolism. These metabolome responses are supposed to maintain in short-term (10 min) treatment with PSI-6130. Thus, inhibition of HCV RNA replication by PSI-6130 under the conditions used may lead to increase in the cytoplasmic ATP level. It is likely that these metabolome responses were not observed after the longer-term (2 h) treatment presumably because the viral replication was inhibited by the inhibitor for a sufficient period of time. Further study is required to address the molecular mechanism underlying change in ATP balance caused by HCV replication and the viral inhibitors.

The mechanism by which ATP accumulates at potential sites of HCV RNA replication remains unclear. We have previously demonstrated that creatine kinase B (CKB), which is an ATP-generating enzyme and maintains cellular energy stores, accumulates in the HCV RC-rich fraction of viral replicating cells [22]. Our earlier results suggest that CKB can be directed to the HCV RC via its interaction with the HCV NS4A protein and thereby functions as a positive regulator for the viral replicase by providing ATP [22]. One may hypothesize that recruitment of the ATP generating machinery into the membrane-associated site, through its interaction with viral proteins comprising the RC, is at least in part linked with elevated concentrations of ATP at a particular site. Through our preliminary study, however, subcellular ATP distribution was not changed significantly in replicon cells where HCV RNA replication was reduced ~50% by siRNA-mediated knockdown of the CKB gene (data not shown). Another possibility

may be implication of communication between mitochondria and membrane-enclosed structures of HCV RC in ATP transport through membrane-to-membrane contact. As indicated in Figure S5, putative sites of the viral RNA replication with high Venus/CFP ratios were mainly localized proximal to mitochondria. Studies are ongoing to understand the mechanism(s) underlying this phenomenon, as well as to determine if changes in ATP levels at intracellular sites supporting replication might also be observed for other RNA or DNA viruses.

In summary, we have used a FRET-based ATP indicator called ATeam to monitor ATP levels in living cells where viral RNA replicates by designing HCV replicons harboring wild-type or mutated ATeam probes inserted into the C-terminal domain of NS5A. We evaluated changes in ATP levels during HCV RNA replication and demonstrated elevated ATP levels at putative sites of replication following detection of FRET signals, which appeared as dot-like foci within the cytoplasm. The ATeam system may become a powerful tool in microbiology research by enabling determination of subcellular ATP localization in living cells infected or associated with microbes, as well as investigation of the regulation of ATP-dependent processes during the lifecycle of various pathogens.

Materials and Methods

Chemicals

PSI-6130 (β-D-2′-Deoxy-2′-fluoro-2′-*C*-methylcytidine) and recombinant human IFN-alpha2b were obtained from Pharmasset Inc. (Princeton, NJ) [23,24] and Schering-Plough (Kenilworth, NJ), respectively. OliA and 2DG were purchased from Sigma-Aldrich (St. Louis, MO). ATP used in this study was complexed with equimolar concentrations of magnesium chloride before use in the experiments.

Plasmids

The construction of the ATeam plasmids pRSET-AT1.03, pRSET-AT1.03^{YEMK} and pRSET-AT1.03$^{R122K/R126K}$, which express wild-type ATeam (AT1.03), as well as a high-affinity mutant (AT1.03^{YEMK}) and a non-binding mutant (AT1.03^{RK}), has been previously described [2]. pHH/SGR-Luc (also termed SGR/luc) contains cDNA of a subgenomic replicon of HCV JFH-1 isolate (genotype 2a; [14]) with firefly luciferase flanked by the Pol I promoter and the Pol I terminator, yielding efficient RNA replication upon DNA transfection [26]. pHH/SGR-Luc/GND (also termed SGR/luc-GND), in which a point mutation of the GDD motif of the NS5B was introduced in order to abolish RNA-dependent RNA polymerase activity, was used as a negative control. pHH/SGR (also termed SGR) was created by deleting the luciferase gene in pHH/SGR-Luc. To generate a series of SGR-ATeam plasmids, wild-type or mutant ATeam genes were inserted into pHH/SGR-Luc or pHH/SGR at the Xho I site of NS5A (between amino acids 418 and 419) [25]. The ATeam genes were also inserted into the same site of pCAGNS5A, which contains the NS5A gene of JFH-1 downstream of the CAG promoter and hemagglutinin (HA) tag [26], yielding NS5A-ATeam plasmids. To generate a plasmid expressing NS3-NS5B-AT1.03 under the control of the CAG promoter, a DNA fragment containing the coding region of NS3/NS4A/NS4B/NS5A-AT1.03/NS5B of SGR/luc-ATeam was inserted into the pCAGGS vector [40]. Exact cloning strategies are available upon request.

Cell culture and plasmid transfection

Human hepatoma Huh-7 cells were propagated in Dulbecco's modified Eagle's medium (DMEM) supplemented with 10% fetal calf serum (FCS) as well as minimal essential medium non-essential amino acid (MEM NEAA)(Invitrogen, Carlsbad, CA) in the presence of 100 units/ml of penicillin and 100 μg/ml of streptomycin. The Huh-7-derived cell lines JFH-1/4-1 and JFH-1/4-5, which support replication of SGR RNA of HCV JFH-1 (genotype 2a) and NK5.1/0-9, which carries the SGR RNA of Con1 NK5.1 (genotype 1b), were cultured and maintained under previously described conditions [15]. DNA transfection was performed using a TransIT-LT1 transfection reagent (Takara, Shiga, Japan) in accordance with the manufacturer's instructions.

CE-TOF MS analysis

Huh-7 cells were mock-infected or infected with HCVcc derived from a wild-type JFH-1 isolate at a multiplicity of infection of 1. When most cells had become virus positive, as confirmed by immunofluorescence, with no observable cell damage at 9 days post-infection, equal amounts of cells with and without HCV infection were scraped with MeOH including 10 μM of an internal standard after washing twice with 5% mannitol solution. Replicon cells (JFH-1/4-5) that were cultured in the absence of G418 for 2 days were harvested and prepared as above. The extracts were mixed with chloroform and water, followed by centrifugation at 2,300× *g* for 5 min at 4°C. The upper aqueous layer was centrifugally filtered through a 5-kDa cutoff filter to remove proteins. The filtrate was lyophilized and dissolved in water, then subjected to CE-TOF MS analysis. CE-TOF MS experiments were performed using an Agilent CE-TOF MS system (Agilent Technologies, Waldbronn, Germany) as described previously [41].

ATP consumption assay

The ATP consumption assay using permeabilized replicon cells was carried out as previously described [13,22] with slight modifications, so that it was unnecessary to add either exogenous phosphocreatine or creatine phosphokinase to minimize ATP reproduction in cells. Cells (2×10^6) cultured in the presence or absence of PSI-6130 for 72 h were treated with 5 μg Actinomycin D/ml, followed by trypsinization and 3 washes with cold buffer B (20 mM HEPES-KOH [pH 7.7], 110 mM potassium acetate, 2 mM magnesium acetate, 1 mM EGTA, and 2 mM dithiothreitol). The cells were permeabilized by incubation with buffer B containing 50 μg/ml digitonin for 5 min on ice and the reaction was stopped by washing 3 times with cold buffer B. The permeabilized cells (1×10^5) were resuspended with 100 μl buffer B containing 5 μM ATP, GTP, CTP, and UTP, 20 μM $MgCl_2$, and 5 μg/ml Actinomycin D. After incubation at 27°C for 15 min, samples were centrifuged, and 20 μl of the supernatant was then mixed with 5 μl of 5× passive lysis buffer (Promega, Madison, WI). The ATP level was determined using a CellTiter-Glo Luminescent cell viability assay system (Promega). All assays were performed at least in triplicate.

Live cell microscopy

Plasmids carrying the ATP indicators were transfected at 48 h (ATeam and NS5A-ATeam) or 4 days (SGR-ATeam) before imaging of the cells. One day before imaging, the cells were seeded onto 30-mm glass-bottomed dishes (AGC Techno Glass, Chiba, Japan) at about 60% confluency. For imaging, the cells were maintained in phenol red-free DMEM containing 20 mM HEPES-KOH [pH 7.7], 10% FCS and MEM NEAA.

Two kinds of confocal microscopies were used to perform the FRET analysis in this study as follows. Since the ways of acquisition of each spectrum were quite different between the two microscopies, differences in the values of the Venus/CFP ratios in different

experiments were observed. In Figures 2, 4B and S2, cells were imaged using a confocal inverted microscope FV1000 (Olympus, Tokyo, Japan) equipped with an oil-immersion 60× Olympus UPlanSApo objective (NA = 1.35). Cells were maintained on the microscope at 37°C with a stage-top incubation system (Tokai Hit, Shizuoka, Japan). Cells were excited by a 405-nm laser diode, and CFP and Venus were detected at 480–500 nm and 515–615 nm wavelength ranges, respectively. In the analysis shown in Figures 5, 6, S3, S4 and S5, FRET images were obtained using a Zeiss LSM510 Meta confocal microscope with an oil-immersion 63× Zeiss Plan-APOCHROMAT objective (NA = 1.4)(Carl Zeiss, Jena, Germany). Cells were maintained on the microscope at 37°C with a continuous supply of a 95% air and 5% CO_2 mixture using a XL-3 incubator (Carl Zeiss). Cells were excited by a 405-nm blue diode laser, and emission spectra of 433–604 nm wavelength range were obtained using an equipped scanning module (META detector) [42,43]. Images were computationally processed by a linear unmixing algorithm using the reference spectrum of CFP and Venus, which were obtained from individual fluorescence-expressing cells. All image analyses were performed using MetaMorph (Molecular Devices, Sunnyvale, CA). Fluorescence intensities of cytoplasmic areas in NS5A-ATeam transfected cells were calculated by subtraction of the signal intensities of the nucleus from the signal intensities of the whole cell, which was standardized by the area of the corresponding cytoplasmic region. Fluorescence intensities of cytoplasmic areas and at dot-like structures corresponding to the putative viral replicating sites in SGR-ATeam-transfected cells were measured and calculated as follows. All pixels above CFP intensity levels of 100–200 were selected. The positions of dot-like structures were then determined by examining areas greater than 0.5×10^{-12} square meters and the intensity of each dot was measured. The fluorescence intensity of the cytoplasmic area, excluding that of the putative viral replicating sites in each cell, was calculated by subtraction of the signal intensities of the nucleus and the dot-like structures, as determined above, from the signal intensity of the whole cell, which was standardized by the area of the corresponding cytoplasmic region. Each Venus/CFP emission ratio was calculated by dividing pixel-by-pixel a Venus image with a CFP image.

To investigate the relationship between Venus/CFP ratios and ATP concentrations in cells, calibration procedures were performed according to previous reports [29,30]. Huh-7 cells were transfected with NS5A-AT1.03 or NS5A-AT1.03^{YEMK}. Forty-eight hours later, the cells were permeabilized by incubation with buffer B containing 50 μg/ml digitonin for 5 min at room temperature. The reaction was stopped by washing 3 times with buffer B, followed by the addition of known concentrations of ATP in warmed medium for imaging. FRET analysis, with calibration of the signal intensity in the cytoplasm of each cell, was performed as described above. Plots were fitted with Hill equations with a fixed Hill coefficient of 2; $R = (R_{max}-R_{min})\times[ATP]^2/([ATP]^2+Kd^2)+R_{min}$, where R_{max} and R_{min} are the maximum and minimum fluorescence ratios, respectively and Kd is the apparent dissociation constant.

To analyze the effect of an inhibitor against HCV NS5B polymerase, the medium for the cells replicating SGR-ATeam was changed to medium containing various concentrations of PSI-6130. After 10-min incubation at 37°C under a continuous supply of 95% air and 5% CO_2, fluorescence intensities of cytoplasmic areas and at dot-like structures were determined as described above. Medium containing 0.01% DMSO was used as a negative control.

To visualize mitochondria, MitoTracker Red CMXRos (Molecular Probes, Eugene, OR) was added to the culture medium to a final concentration of 100 nM, incubated for 15 min at 37°C and the cells were then washed twice with phosphate buffered saline (PBS) before FRET analysis of living cells. Images were computationally processed as described above. The reference spectrum of MitoTracker Red CMXRos was obtained from stained parental, non-transfected, Huh-7 cells.

Indirect immunofluorescence

Cells expressing SGR-ATeam were cultured in 30-mm glass-bottomed dishes with an address grid on the coverslip (AGC Techno Glass). After FRET analysis of living cells as described above, the cells were fixed with 4% paraformaldehyde at room temperature for 30 min. After washing with PBS, the cells were permeabilized with PBS containing 0.3% Triton X-100 and individually stained with a rabbit polyclonal antibody against NS3 [44], an anti-NS5A antibody [45], or a mouse monoclonal antibody against dsRNA antibody (Biocenter Ltd., Szirak, Hungary) [46]. The fluorescent secondary antibody used was Alexa Fluor 555-conjugated anti-rabbit- or anti-mouse IgG (Invitrogen). The cells were imaged using a Zeiss LSM510 Meta confocal microscope with an oil-immersion 63× Zeiss Plan-APOCHROMAT objective (NA = 1.4). For dual-color imaging, the ATeam signal was excited with the 488-nm laser line of an argon laser and Alexa Fluor 555 was excited with a 543-nm HeNe laser under MultiTrack mode. Emission filters with a 505- to 530-nm band-pass and 560-nm-long pass filter were used.

Luciferase assay

Huh-7 cells transfected with SGR/luc or SGR/luc-ATeam were harvested at different time points after transfection (Figure 4D) or at 3 days after treatment with PSI-6130 (Figure S6) and lysed in passive lysis buffer (Promega). To monitor HCV RNA replication, the luciferase activity in cells was determined using a Luciferase Assay system (Promega). All assays were performed at least in triplicate.

MTT assay

Cell viability was assessed using the Cell Proliferation Kit II (Roche, Indianapolis, IN) according to the manufacturer's instructions. The kit measures mitochondrial dehydrogenase activity, which is used as a marker of viable cells, using a colorimetric sodium3'-[1(-phenylaminocarbonyl)-3,4-tetrazolium]-bis(4-methoxy-6-nitro)benzene sulfonic acid hydrate (MTT) assay.

Quantification of HCV RNA

HCV RNA copies in the replicon cells with or without PSI-6130 treatment were determined using the real-time detection reverse transcription polymerase chain reaction (RTD-PCR) described previously [47] with the ABI Prism 7700 sequence detector system (Applied Biosystems Japan, Tokyo, Japan).

Western blotting

The proteins were transferred onto a polyvinylidene difluoride membrane (Immobilon; Millipore, Bedford, MA) after separation by SDS-PAGE. After blocking, the membranes were probed with a rabbit polyclonal anti-NS5A antibody [44], a rabbit polyclonal anti-NS5B antibody (Chemicon, Temecula, CA), or a mouse polyclonal anti-beta-actin antibody (Sigma-Aldrich), followed by incubation with a peroxidase-conjugated secondary antibody and visualization with an ECL Plus Western blotting detection system (GE Healthcare, Buckinghamshire, UK).

Supporting Information

Figure S1 ATP Levels in HCV replicon cells and parental Huh-7 cells determined by CE-TOF MS. ATP metabolites in Huh-7 cells and JFH-1/4-5 cells were measured by